minerals

MDPI

Article

The Effect of K-Fertilization and Irrigation on the Composition of Cultivated Soils: Examples from Israel

Amir Sandler [1,*], Pinchas Fine [2] and Asher Bar-Tal [2]

[1] Geological Survey of Israel, 32 Yesha'ayahu Leibowitz, Jerusalem 9692100, Israel
[2] Institute of Soil, Water and Environmental Sciences, Agricultural Research Organization, Volcani Institute, 68 HaMacabim Rd., Rishon Lezion 7505101, Israel; finep@volcani.agri.gov.il (P.F.); abartal@volcani.agri.gov.il (A.B.-T.)
* Correspondence: sandler@gsi.gov.il

Abstract: Evaluation of soil sustainability should take into account chemical and mineralogical changes due to cultivation. Potassium (K) application is a key farming practice that may potentially affect phyllosilicate composition and soil properties. Irrigation is another agent that affects soil composition. This study aims to evaluate the imprints of cultivation on the chemical and mineralogical compositions of lowland soils under semi-arid and Mediterranean climate regimes and to assess them with the natural pedogenesis. The sites examined include two permanent plot experiments with crop rotation, and three single-plant plots. Cultivated, control, and fallow soils were analyzed for their chemical and mineralogical composition. The X-ray diffraction patterns of the clay fraction were decomposed to achieve quantitative detection of changes among the illite–smectite (IS) phases and in kaolinite amounts. In loamy and clayey soils dominated by IS phases, cultivation caused minor changes and diverse behavior of the IS phases. Yet, the K balance was negative under high fertilization levels and higher plant mass production. Fertilization enhanced the natural process of transforming IS into kaolinite and illite in the sandy soil, leading to a positive K balance. This study emphasizes the importance of IS minerals as a dynamic K pool that responds to plant needs.

Keywords: soil; chemical composition; mineralogical composition; phyllosilicates; potassium; permanent plots; Israel

Citation: Sandler, A.; Fine, P.; Bar-Tal, A. The Effect of K-Fertilization and Irrigation on the Composition of Cultivated Soils: Examples from Israel. *Minerals* **2023**, *13*, 1547. https://doi.org/10.3390/min13121547

Academic Editor: Barbara Kalisz

Received: 9 October 2023
Revised: 3 December 2023
Accepted: 11 December 2023
Published: 14 December 2023

1. Introduction

Fertilization and irrigation used in conjunction with intensive soil cultivation have the potential to alter soil properties over time. The stability of the soil's constituents and the rate of pedogenic processes are mainly impacted by the soil moisture regime and chemical environment. Soil mineralogical composition is one of the critical parameters that affect cultivation, especially the phyllosilicate transformation and neoformation by leaching silicon and aluminum, and uptake and release of potassium (K), an essential plant nutrient. Accordingly, in order to achieve optimal production of sustainable soil, K management must be cautiously controlled [1,2]. If the harvested K is not replaced by K released from soil minerals or K fertilizers a negative balance prevails, depleting the soil-available K [3]. Besides optimizing plant production, the addition of K-fertilizers may also improve soil structure and water retention [4,5]. However, K application in excess may cause a reduction in soil pore size that lowers the hydraulic conductivity [6].

A simplified classification of K occurrence in soil is into four groups: water-extractable, exchangeable (adsorbed), slowly exchangeable, and structural forms [7,8]. Most of the soil K generally occurs as structural K in the primary minerals K-feldspars, biotite, and muscovite and is only available to plants through mineral weathering [9]. Structural K has been thought to be of relatively little significance for short-term plant K nutrition [10,11]; however, in the long term, it may play a substantial role in K supply [11–14]. Water-extractable K and exchangeable K are readily available to plants but typically make up only a small portion of soil K [15] (and references therein). Secondary soil minerals promote reversible K release and fixation, especially the slowly exchangeable K fixed in 2:1 mixed-layer phyllosilicate interlayer sites, namely, illite–smectite (IS) [2,8,16]. The IS phases are acknowledged as the key components for K uptake by plants and, accordingly, for agricultural production [17,18]. The chemical formula of IS is variable, reflecting its position on the smectite-to-illite continuity line. For example, $K_{0.28}Ca_{0.12}(Al_{1.56}Fe^{3+}{}_{0.16}Mg_{0.31})[(Si_{3.70}Al_{0.30})O_{10}(OH)_2]$ is relatively smectitic and $K_{0.62}Ca_{0.05})\ Al_{1.78}Fe^{3+}{}_{0.02}Mg_{0.25})[(Si_{3.39}Al_{0.61})O_{10}(OH)_2]$ is relatively illitic.

Short-term changes in soil 2:1 phyllosilicate structure and composition due to K-fertilization over a number of years and even from season to season have been distinguished by X-ray diffraction (XRD) [4,19–21]. The reported changes are frequently minor, and the challenge of quantifying them by XRD led to the use of modeling simulations [9,18,22,23] or peak decomposition (deconvolution) techniques [11,17,24,25].

The current study aims to detect potential chemical and mineralogical changes in long-term intensively cultivated soils in Israel. The soils selected for the study are lowland IS-rich soils under semi-arid and Mediterranean climates, which have been irrigated and fertilized by K, nitrogen (N), and phosphorous (P). The lowland soils, where the majority of farming in Israel takes place, include the loess plains of the northwestern Negev, the sandy coastal plain along the Mediterranean Sea, the parallel alluvial plains between the coastal plain and the backbone mountains, and the northern valleys of the intra-mountainous range. Except for the sandy soils of the coastal plain, most cultivated lowlands soils are loamy or clayey. The current study had the opportunity to use two previous permanent plot experimental farms' soil samples. The initial goal of the experiments was to maximize crop fertilization levels; however, soil K and mineralogy investigations have not yet been carried out. Other active farming sites that were chosen because of their high K application were also studied.

In addition to the major IS phases, kaolinite ($Al_2Si_2O_5(OH)_4$) is a minor (<25%) constituent in lowland soils of Israel, but in the sandy soils of the coastal plain it can, locally, become the major phyllosilicate. Illite ($K_{0.65}Al_{2.0}[Al_{0.65}Si_{3.35}O_{10}](OH)_2$) amounts are small but variable (<15%), chlorite (clinochlore $Mg_5Al(AlSi_3O_{10})(OH)_8$) is detectable in trace amounts (<5%), and palygorskite ($(Mg,Al)_2Si_4O_{10}(OH){\cdot}4H_2O$) may be present in small amounts in arid soils [26]. The origin of the fine fractions of the soil in Israel is dust arriving from the Sahara and Arabian deserts [27,28]. In Israel and neighboring countries, pedogenesis promotes the transformation of phyllosilicates in response to local environmental conditions [29–32]. The major transformation takes place under the Mediterranean climate where illitic IS phases of dust gradually become more smectitic and approach smectite dominance in vertisols. Another transformation route occurs under intensive leaching, especially in porous and well-structured soils, in which IS phases may transform into both kaolinite and illite [33,34].

Hardly any attention has been accounted for by previous studies on the relations of mineralogical and chemical changes brought on by farming with the underlying long-term pedogenic processes, such as the dissolution of primary minerals and calcite, and the subsequent transformation and dissolution/precipitation processes within the soil. In the last decade, there has been an increasing number of studies that use soil archives of long-term experiments, most of them are from the northern hemisphere, mainly the USA and UK, but none are from the Mediterranean region [35]. Moreover, most studies reported changes in SOM and macronutrients [35], whereas only a few studies investigated possible changes in the mineralogy of the soils. In Israel, studying the long-term impact of fertilization on soil productivity and nutrient balances has been performed on two permanent experimental plot stations [36]. Soil chemical analyses during the experiments included available forms of fertilizers (K, N, P) and a few additional ions. No study has examined the effects of long-term farming on the mineralogy of the clay fraction and the bulk mineralogical and chemical compositions. Accordingly, the objectives of the current study were to (1) identify the effects of irrigation and fertilization on lowland soils in Israel, with a focus on the soil K balance and (2) assess the potential relations of agricultural changes with the natural pedological evolution of soils.

2. Materials and Methods

2.1. Sampling Sites

The five sampling sites are presented in Figure 1. Two sites are the experimental stations in Gilat and Bet Dagan of The Agricultural Research Center of Israel. Fertilization studies were conducted there in permanent plots with crop rotation occurring for more than thirty years. Three additional single-crop plots were a tomato plot on sandy soil (Mishmeret) in the Coastal Plain where intensive fertilization, including sheep manure, has been carried out for ten years; a banana plantation (Nir Etzion) in the Carmel Mountain's foothills where fertilizing with higher than usual amounts of K has been carried out for fifty years; and a fifteen-year-old grapefruit orchard (Sarid) in the northern valleys, including eight years of irrigation by effluents. The basic data of the sites studied are presented in Table 1 and additional information is presented below.

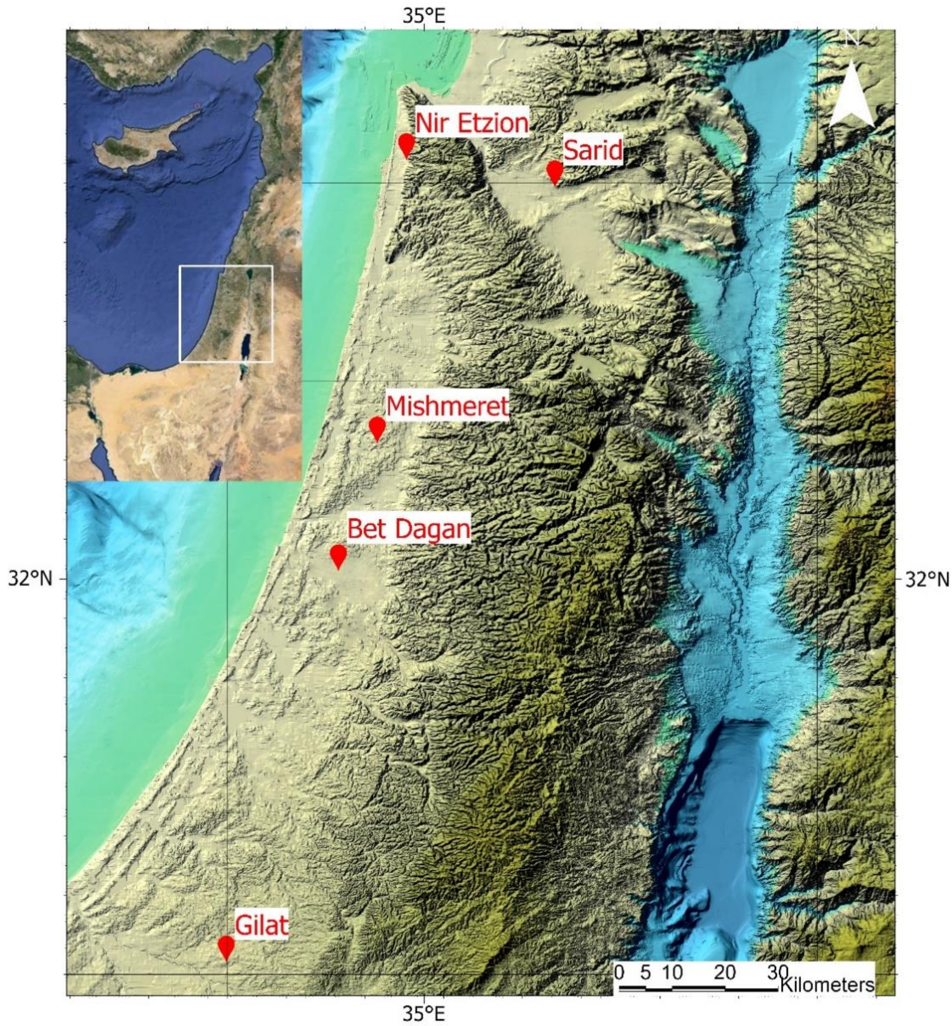

Figure 1. The location of the five sampling sites is displayed on a relief map. The study area is framed on the inset Levant relief map.

Table 1. Basic data of the five sites studied: two sites of experimental permanent plots and three sites of single-plant plots. Each soil type includes the USDA taxonomy and the Israeli classification names.

Site Name	Geography/ Geomorphology	Coodinations		Cultivation	Years	Soil Type	pH	Texture	m.a.p.*	Elevation
		E	N						mm	m a.s.l.
Gilat	Northwestern Negev; loessial plain	31.3531	34.6649	Experimental plots	1961–1994	Calcic Haploxeralf (Loamy Loess)	8.2	Loam	275	175
Bet Dagan	Eastern Coastal Plain; alluvial plain	32.0124	34.8549	Experimental plots	1961–1993	Chromic Haploxerert (Vertisol)	7.8	Silty clay	600	30
Mishmeret	Coastal Plain; sand plain	32.2276	34.9209	Private farm; tomatoes	1965–2009	Typic Rhodoxeralf (Hamra)	7.5	Loamy sand	600	70
Nir Etzion	Mt. Carmel foothills; alluvial plain	32.7050	34.9704	Kib. banana plant	1958–2008	Typic Chromoxeret (Vertisol)	8.0	Clay	625	30
Sarid	Yizre'el Valley; margins of alluvial plain	32.6589	35.2220	Kib. grapefruit orchard	1992–2007	Typic Chromoxeret	7.9	Clay	500	80

* m.a.p. = mean annual precipitation 1961–1990; Kib. = kibbutz.

2.1.1. Gilat Permanent Plot Experiment

The main objective of the experiment was to measure the yields of various field crop rotation systems on irrigated deep loess soil as affected by the long-term cumulative application of various combinations of N fertilizer and organic manure. Four levels of cultivation of N fertilizer were applied: a control without N fertilizer, and three dozes with constant ratios of 100%, 200%, and 300% in which the absolute value of the 100% dose was fit to the type of crop that was grown in rotation, labeled: N0, N1, N2, N3, and three organic manure treatments labeled M0 (no organic manure), M1 (dairy manure 30 t/ha), M2 (dairy manure 90 t/ha), and R (city refuse compost 30 t/ha) were applied. The samples selected for the current study are of the N and manure application and are listed in Table 2a. All plots received basic K and variable P fertilization (Table 2a); the various manure levels introduced also added variable concentrations of K and P. The following crops were rotated in the first years: sugar beets, corn, onions, potatoes, wheat, and onions, and later on other crops [36]. Fallow soil was sampled for the current study.

Table 2. A list of the samples studied, the various soil types, and the levels of fertilization.

(2a) Gilat.				
Lab No.	**Type**	**Plot**	**Year**	**Fertilizers ***
0–20 cm				
F0–20	Fallow		2006	-
F1 0–20	Fallow		2008	-
F2 0–20	Fallow		2008	-
D	Control	24	1987	M0, N0
E	Control	24	1987	M0, N0
G	Control	21	1987	M0, N0
J	Control	38	1987	M0, N0
A		3	1987	M0, N3
C		18	1987	M2, N0
H		34	1987	M2, N0
L		43	1987	M2, N0
N		92	1987	M2, N0
B		13	1987	M2, N3
I		36	1987	M2, N3
K		42	1987	M2, N3
M		57	1987	M2, N3

Table 2. *Cont.*

(2a) Gilat.				
Lab No.	**Type**	**Plot**	**Year**	**Fertilizers ***
20–40 cm				
F 20-40	Fallow		2006	-
F1 20-40	Fallow		2008	-
F2 20-40	Fallow		2008	-
Q	Control	21	1987	M0, N0
R	Control	24	1987	M0, N0
U	Control	38	1987	M0, N0
P		18	1987	M2, N0
S		34	1987	M2, N0
W		43	1987	M2, N0
Y		92	1987	M2, N0
O		13	1987	M2, N3
T		36	1987	M2, N3
V		42	1987	M2, N3
X		57	1987	M2, N3

* N3 = 120–390 kg N ha^{-1} annual rate, 6450 kg N ha^{-1} 1963–1987 (accumulated); M2 = 0–720 kg (Organic N) ha^{-1} annual rate, 5520 kg (Organic N), ha^{-1} + 7200 kg K ha^{-1} 1963–1987 (accumulated); K was applied as KCl 0–230 kg, 2390 kg ha^{-1} K 1963–1987 (accumulated); P = 0–100 K ha^{-1} highly variable annual rates. M—manure; N—nitrogen.

(2b) Bet Dagan.					
Lab No.	**Type**	**Block**	**Plot**	**Year**	**Fertilizers ***
0–20 cm					
F1 0-20	Fallow			2006	-
F2 0-20	Fallow			2006	-
F3 0-20	Fallow			2006	-
A	Control	III	9	1965	[N,P,K]0
B	Control	III	9	1993	[N,P,K]0
G	Control	II	73	1995	[N,P,K]0
J	Control	III	9	1963	[N,P,K]0
K	Control	III	9	1996	[N,P,K]0
AE		I	41	1993	N3, P4, K0 + gM
AF		I	76	1996	N3, P4, K0 + gM
AG		V	80	1996	N3, P4, K0 + gM
C		I	85	1993	N4, P4, K2
D		V	89	1993	N4, P4, K2
H		II	86	1964	N4, P2, K2
I		II	86	1995	N4, P2, K2
L		III	20	1963	N4, P3, K2
M		III	20	1995	N4, P3, K2
N		IV	25	1963	N4, P3, K2
O		IV	25	1995	N4, P3, K2
V		V	44	1996	N4, P4, K2 + M
W		I	15	1996	N4, P4, K2 + M
Y		II	41	1996	N4, P4, K2 + M
Z		III	40	1996	N4, P4, K2 + M

Table 2. *Cont.*

(2b) Bet Dagan.					
Lab No.	**Type**	**Block**	**Plot**	**Year**	**Fertilizers ***
20–40 cm					
F1 20-40	Fallow			2006	-
F2 20-40	Fallow			2006	-
F3 20-40	Fallow			2006	-
P	Control	II	73	1995	[N,P,K]0
Q	Control	III	9	1996	[N,P,K]0
R		III	20	1995	N4, P3, K2
S		IV	25	1995	N4, P3, K2
T		II	86	1995	N4, P2, K2
AB		I	15	1996	N4, P4, K2 + M
AC		II	41	1996	N4, P4, K2 + M
AD		III	40	1996	N4, P4, K2 + M

* N0, N3 and N4 = 0, 180 and 240 kg N ha^{-1} annual rate, P0, P3 and P4 0, 36, 72 kg P ha^{-1} annual rate, K0 and K2 = 0 and 320 K ha^{-1} annual rate; M—manure; N—nitrogen; P—phosphorous; K—potassium; gM—green manure.

(2c) Mishmeret.			
Lab no.	**Type**	**Year**	**Fertilizers ***
0–20 cm			
YTF	Fallow	2008	-
YTF a	Fallow	2008	-
YTF b	Fallow	2008	-
YT 1	Tomatoes	2008	Fert. + M
YT 1a	Tomatoes	2008	Fert. + M
YT 1b	Tomatoes	2008	Fert. + M
5–20 cm			
YTG	Grass lawn	2009	-
YTG a	Grass lawn	2009	-
YTG b	Grass lawn	2009	-
20–40 cm			
YTF	Fallow	2008	-
YTF a	Fallow	2008	-
YTF b	Fallow	2008	-
YT 1	Tomatoes	2008	Fert. + M
YT 1a	Tomatoes	2008	Fert. + M
YT 1b	Tomatoes	2008	Fert. + M
YTG	Grass lawn	2009	-
YTG a	Grass lawn	2009	-
YTG b	Grass lawn	2009	-

* N = 180 kg N ha^{-1} annual rate as KNO_3 and $Ca(NO_3)_2$; K = 464 kg K ha^{-1} annual rate as KNO_3 + 15 m^3 manure; Fert.—K and N fertilizers; M—sheep manure.

Table 2. *Cont.*

(2d) Nir Etzion.			
Lab no.	**Type**	**Year**	**Fertilizers ***
0–20 cm			
NE a	Banana 1	2008	Fert.
NE b	Banana 2	2008	Fert.
NE c	Banana 3	2008	Fert.
NE d	Olive 1	2008	-
NE e	Olive 2	2008	-
NE f	Field 1	2008	?
NE g	Field 2	2008	?
NE h	Field 3	2008	?
20–40 cm			
NE i	Banana 1	2008	Fert.
NE j	Banana 2	2008	Fert.
NE k	Banana 3	2008	Fert.
NE l	Olive 1	2008	-
NE m	Olive 2	2008	-
NE n	Field 1	2008	?
NE o	Field 2	2008	?
NE p	Field 3	2008	?

* N = 500 kg ha^{-1} annual rate; K = 1500 kg ha^{-1} annual rate; Fert.—K and N fertilizers; ?—unknown fertilization.

(2e) Sarid.			
Lab no.	**Type**	**Year**	**Fertilizers ***
0–20 cm			
F1 N 0-20	Fallow	2007	-
F2 N 0-20	Fallow	2007	-
F3 N 0-20	Fallow	2007	-
A		2007	Effluent + Compost + KCl
B		2007	Effluent + Compost + KCl
C		2007	Effluent + Compost + KCl
20–40 cm			
F1 20-40	Fallow	2007	-
F2 20-40	Fallow	2007	-
F3 20-40	Fallow	2007	-
D		2007	Effluent + Compost + KCl
E		2007	Effluent + Compost + KCl
G		2007	Effluent + Compost + KCl

* Estimated annual rates: N = 170 kg ha^{-1}; K = 275 kg ha^{-1}; P = 110 kg ha^{-1}.

2.1.2. Bet Dagan Permanent Plot Experiment

The main objective of the experiment was to measure the yields of various field crop rotation systems on irrigated deep alluvial soil as affected by long-term cumulative application of various combinations of N, P, K fertilizers, and organic manure. The following four factors were investigated: (a) five levels of N fertilizer, 0, 60, 120, 180, and 240 kg N ha^{-1}, labeled N0, N1, N2, N3, N4; (b) five levels of P fertilizer, 0, 9, 18, 36, and 72 kg P ha^{-1}, labeled P0, P1, P2, P3, P4; (c) three levels of K fertilizer, 0, 160, and 320 kg K ha^{-1}, labeled K0, K1, K2; organic manure treatments of farmyard, or dairy manure or green manure, usually pea (Table 2b). The following crops were rotated in the first years: wheat, chickpea, sugar beet, oats, cotton, and sorghum. Fallow soil was sampled for the current study. In the permanent plot stations K was determined only as the available K concentration by the $NaHCO_3$ 0.5 M extract method [36,37].

2.1.3. Mishmeret

The field has been cultivated for decades as part of a private farm. In the past ten years before sampling, the farmer has been growing tomatoes and continuously fertilizing them with sheep manure from a nearby pen (Table 2c). The nearby grass lawn was also sampled in order to compare an irrigation-only regime with an irrigation-and-fertilization regime. Additionally, fallow soil was sampled.

2.1.4. Nir Etzion

This kibbutz banana plantation was chosen to test the effect of intensive fertilization on a single-cropped soil for about fifty consecutive years before sampling. Because banana plants consume about 1100 kg of K per ha^{-1}, the fertilization contains a higher dose of this element (Table 2d). Since there are no fallow soils with the same or comparable qualities, samples from a nearby reaped wheat field and an olive grove were taken for comparison. The grove's soil closely resembles fallow soil because it was not farmed for years prior to sampling.

2.1.5. Sarid

This kibbutz grapefruit orchard was planted in 1992 and after four years was experimentally irrigated by treated wastewater for ten years more before sampling. The control plots were irrigated with freshwater but were not examined in the current study. Fallow soil was sampled as well (Table 2e). The annual amounts of fertilizers were evenly estimated.

2.2. Sampling and Sample Processing

Three replicates of topsoil (0–20 cm) and subsoil (20–40 cm) samples were collected for each site and each agricultural category. Analysis was done on dried materials that had been sieved through a 2 mm sieve (bulk fraction). For the determination of the bulk mineralogical and chemical compositions, a portion each of <2 mm fraction was mechanically ground. The <1 μm fraction was selected to represent the clay fraction since it was tested to fully maintain the phyllosilicate composition while lowering the quartz amount and thus improving the preferred orientation (Figure 2).

For the clay fraction analysis, a portion of the bulk fraction was agitated in water for several hours, buffered acetic acid was added, and after the carbonates had completely dissolved, it was washed up and given a brief treatment with low-intensity ultrasound. The <1 μm fraction was separated using Stokes Law once a stable suspension was attained, and it was then saturated with $SrCl_2$. After washing, a thick suspension was pipetted onto glass slides and analyzed after air-drying, glycolation (at least 8 h at 60 °C and cooling overnight), and heating to 550 °C (2 h).

2.2.1. X-ray Diffraction (XRD)

A Philips X-ray diffractometer (1730/1710; Almelo, The Netherlands) was operated with 40 kV and 30 mA, CuKα radiation, 1°, 0.1 mm, 1° slits, and a sealed proportional detector. The bulk mineralogical composition was semi-quantitatively determined on side-loaded powder runs. Semi-quantitative clay composition was calculated from the peak areas of randomly ordered IS (R0), kaolinite, and illite divided by a 4:2:1 factor, respectively [26] (and references therein). The IS expandability was roughly estimated by the saddle value. The higher the saddle value, the higher the amount of interstratified illitic layers. The saddle value measures the ratio between the height from the baseline to the low next to the IS reflection, and the height from the baseline to the top of the IS reflection [26,38]. The bulk and clay fraction results are presented in 5% intervals and sum up to 100 ± 5%.

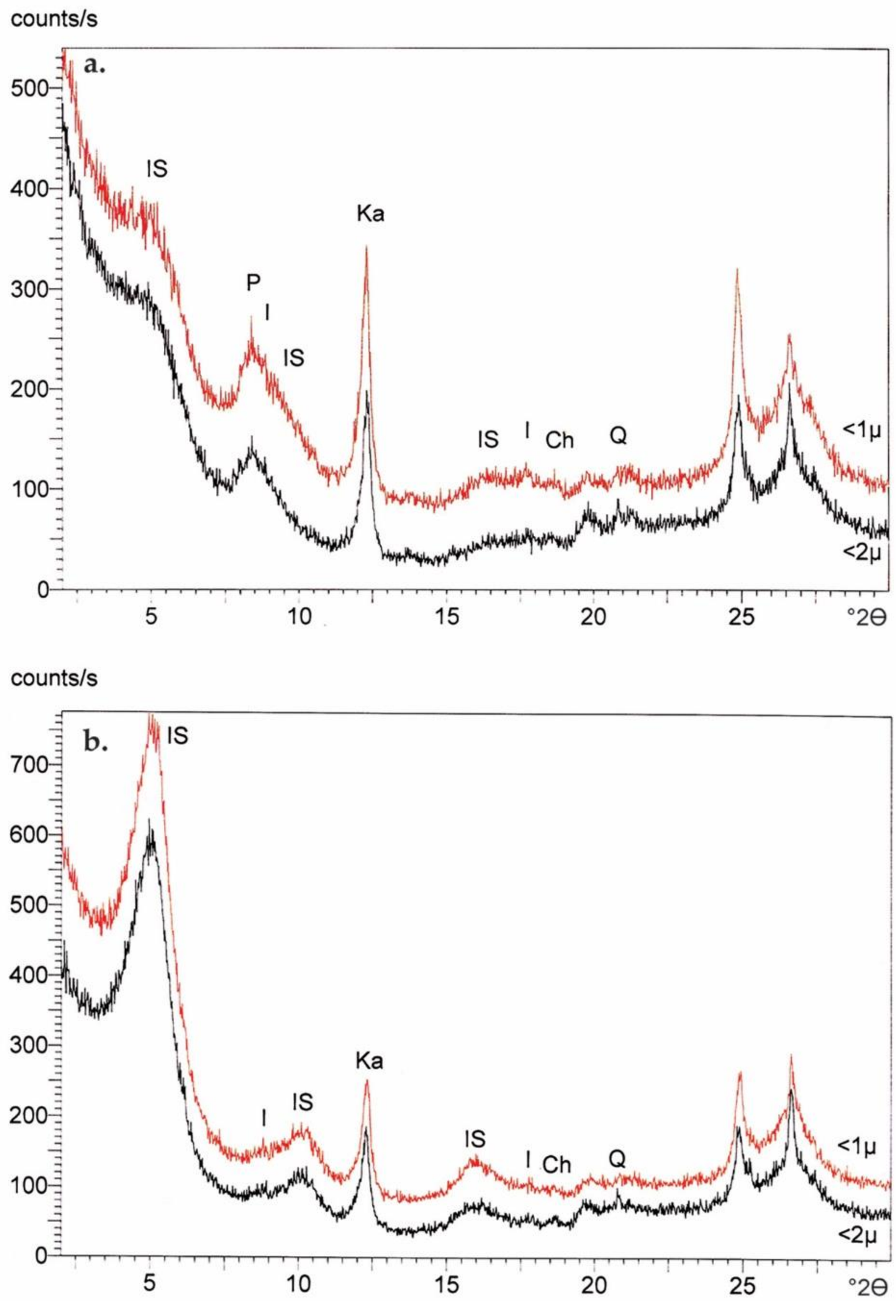

Figure 2. The mineralogical composition (oriented, glycolated) of the clay fraction of (**a**) Gilat and (**b**) Bet Dagan. The diffractograms demonstrate the difference between the clay assemblages of the Gilat and Bet Dagan sites, and the similarity between the <2 and <1 μm fractions. Abbreviations: IS = illite–smectite; p = palygorskite; I = illite; Ka = kaolinite; Ch = chlorite; Q = quartz.

2.2.2. Quantitative Evaluation of the Clay Fraction

The air-dried X-ray patterns were decomposed into their main components using the DecompXR program [39]. Peak areas were determined as the product of peak height and width at half height. The 2:1 phyllosilicates were considered in the following groups: illite with a well (WCI) and a poorly crystallized component (PCI), illite-rich mixed layered (IS), smectite-rich mixed layered (SI), and chlorite (Ch) (Figure 3).

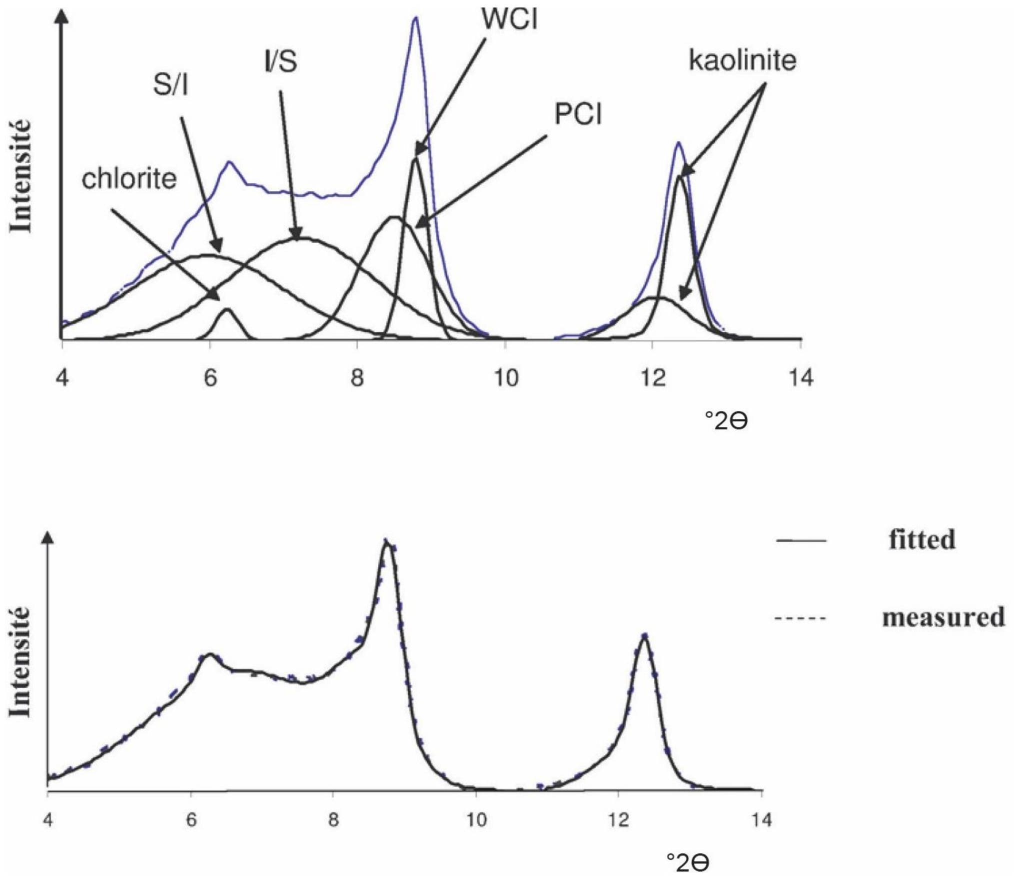

Figure 3. Demonstration of decomposition of a clay fraction diffractogram by the DecompXR program. The components are those used in the current study. S/I = smectitic IS; I/S = illitic IS; PCI = poorly crystallized illite; WCI = well-crystallized illite.

Illite peaks (WCI and PCI) have peak maxima near the 10 Å position, whereas mixed-layered peak positions range from 12 to 15 Å, depending on the relative proportion of illitic layers. Three indicators were calculated and used in this study: **%IS**, which is the ratio of the total areas of the illitic phases WCI, PCI, and IS to the total areas of all 2:1 phases. The center of gravity (**cg**) indicator calculates the weighed position of the (001) of all 2:1 phyllosilicates [16] to provide an estimation of the total amount of illitic layers. These indicators enabled us to compare the change in relative abundance of the potassic clays that are potentially affected by plant growth and fertilizer application. The third indicator is **%K**. It displays the ratio of the area of the kaolinite, on its three sub-components, to the total area of all reflections in the analyzed area, in order to track the potential formation of pedogenic kaolinite. In most cases, the kaolinite reflection can be decomposed into well-ordered kaolinite and less-ordered kaolinite. However, samples from Israel's leached red soils may show asymmetry toward the low angle, necessitating the insertion of a third component that represents a kaolinite–smectite (KaS) mixed-layer phase. Kaolinite in all samples was decomposed into three components for the sake of uniformity, but their relative amounts were not measured.

2.2.3. Chemical Composition

Major element composition of the bulk soil fraction was determined by ICP-OES (Perkin Elmer, OPTIMA 3300, Waltham, MA, USA) after lithium metaborate ($LiBO_2$) fusion of ground sample (0.25 g). Each analysis run included repeated determinations of three of the international standards SO-3, BE-N, BHVO-1, SCo-1, NIM-L, and NIM-G. Errors were <2%.

3. Results

3.1. Bulk Mineralogical Composition

Quartz and phyllosilicates are the major minerals at the four fine-textured sites studied. Quartz is more than twice the amount of phyllosilicates in Gilat and about half the amount of phyllosilicates in Sarid, whereas similar amounts occur in Bet Dagan and Nir Etzion. The quartz amount in the sandy Mishmeret soil is >80% (Table 3). Calcite is a minor mineral whose amount declines from 15%–20% in the semi-arid loess soil to about 10% in the northern sites under the Mediterranean climate, apparently due to the increase in rainfall. Exceptionally, the northernmost Sarid site has a calcite amount of 20%–25%, which is higher than the typical 5%–10% calcium amount of similar nearby soils, e.g., [4,40]. The feldspars group is of minor or trace amounts, declining significantly from south to north (Table 3).

The semi-quantitative results do not allow for distinguishing between fallow and cultivated plots, or between topsoil and subsoil, in any of the sites studied. However, the calcite amount in Gilat is exceptional, as it is on average higher in fallow than in all other cultivated samples due to leaching by irrigation.

Table 3. Bulk mineralogical composition semi-quantitative (%).

Gilat								
Lab No.	**Type**	**Quartz**	**Calcite**	**Dolom.**	**K-Felds.**	**Plagioc.**	**Phyllos.**	**Others**
0–20 cm								
F 0–20	Fallow	45	15–20	<3	10	10	20	Cli.
F1 0–20	Fallow	45	15–20	<2	10	10	15–20	-
F2 0–20	Fallow	55	15–20	<2	5–10	5–10	15–20	-
D	Control	50	15	<2	10	10	15	Am.
E	Control	45–50	15	<2	10–15	10	15–20	-
A	M0, N3	50	15	<2	5	10–15	15–20	Cli.
C	M2, N0	50	10–15	<2	10	10	15	-
N	M2, N0	50	10–15	<3	5	10–15	15–20	Cli. Am.
B	M2, N3	50	15	<3	5–10	5–10	15–20	-
20–40 cm								
F 20–40	Fallow	45	15	<5	10–15	10–15	15	Am.
F1 20–40	Fallow	40–45	15	<5	10	15	15–20	Cli. Am.
F2 20–40	Fallow	55	15	<2	10	10	15	-
Q	Control	45	15	5	10–15	10	15	Cli. Am.
R	Control	50	15	<3	10–15	5–10	15–20	Cli.
U	Control	40–45	10	<2	10	15	15	Am.
P	M2, N0	50	15	<2	5	5–10	15–20	Am.
S	M2, N0	45	10–15	<2	15	15	15	Cli. Am.
W	M2, N0	50–55	15	<5	5–10	15	15	Cli. Am.
Y	M2, N0	45	10–15	<3	5–10	15	20	Am.
O	M2, N3	50–55	15	<2	10	10–15	15	Cli. Am.
T	M2, N3	55	10–15	<3	10–15	5	15	Cli. Am.
V	M2, N3	55	15	<2	5	10–15	15	Am.
X	M2, N3	50–55	10	<2	5	15	20	Cli. Am.

Table 3. *Cont.*

Bet Dagan								
Sample	**Type**	**Quartz**	**Calcite**	**Dolom.**	**K-Felds.**	**Plagioc.**	**Phyllos.**	**Others**
0–20 cm								
F1 0–20	Fallow	40–45	10	<1	5	<5	40–45	-
F2 0–20	Fallow	40	10	<1	5	<5	45	-
F3 0–20	Fallow	40	10	<1	<3	5	45	-
A	Control	40–45	5–10	<1	5–10	5	40	-
B	Control	40–45	10	-	5	5–10	40	-
G	Control	40	10	<1	5–10	<5	40–45	-
J	Control	40	10	<1	5–10	5–10	40–45	Am.
K	Control	45	10	-	<3	5	40–45	Am.
C	N4, P4, K2	40	10	<1	<5	5	40–45	-
D	N4, P4, K2	45	5–10	<1	5	5	40	-
H	N4, P2, K2	40	10	<2	5	<5	45	-
I	N4, P2, K2	40	5–10	-	<5	<5	40–45	Am.
L	N4, P3, K2	40–45	10	-	<5	<5	40–45	-
M	N4, P3, K2	40–45	10	-	5	5–10	40	-
N	N4, P3, K2	40–45	10	<2	5–10	<5	40	-
O	N4, P3, K2	45	10	<1	<5	5	40–45	-
V	N4, P4, K2 + M	40–45	5–10	<1	5	<5	40	-
W	N4, P4, K2 + M	40	10	<1	<5	<5	40	-
Y	N4, P4, K2 + M	45	10	<2	<5	<5	40–45	-
Z	N4, P4, K2 + M	45	5–10	<1	<5	5	40–45	-
20–40 cm								
F1 20–40	Fallow	40–45	10	<1	<5	5	45	Am.
F2 20–40	Fallow	40	10	<1	<5	5	45	-
F3 20–40	Fallow	40	10	<2	<5	5–10	45	-
P	Control	40–45	10	<1	10	5	45	-
Q	Control	35–40	10	<1	5–10	10	40	-
R	N4, P3, K2	40–45	5–10	<1	5–10	10	40–45	Am.
S	N4, P3, K2	35–40	10	-	5–10	10	40	Am.
T	N4, P2, K2	35–40	10	-	5–10	<5	45	-
AB	N4, P4, K2 + M	35–40	10	<1	5	5–10	45	Am.
AC	N4, P4, K2 + M	40	10	<1	5	5	45	Am.
AD	N4, P4, K2 + M	40	10	-	5	<5	45	Am.
Mishmeret								
Sample	**Type**	**Quartz**	**Calcite**	**Dolom.**	**K-Felds.**	**Plagioc.**	**Phyllos.**	**Others**
0–20 cm								
YTF 0–20	Fallow	85	<0.5	<0.5	5	<5	5	-
YTFa 0–20	Fallow	85–90	<0.5	<0.5	<5	<5	5–10	-
YTFb 0–20	Fallow	90	-	-	<3	<5	5	-
YT1	Tomatoes	85–90	<0.5	<0.5	<5	<5	5–10	-
YT1a	Tomatoes	85–90	<0.5	<0.5	<5	<3	5–10	-
YT1b	Tomatoes	85	<0.5	-	<3	5	10	-

Table 3. *Cont.*

Mishmeret								
Sample	**Type**	**Quartz**	**Calcite**	**Dolom.**	**K-Felds.**	**Plagioc.**	**Phyllos.**	**Others**
5–20 cm								
YTG	Grass lawn	85–90	-	<0.5	5	<3	5–10	Gyp.
YTG a	Grass lawn	80	-	-	5	5–10	5–10	Gyp.
YTG b	Grass lawn	80–85	<5	?	5	<3	10	-
20–40 cm								
YTG	Grass lawn	85–90	-	-	<5	<3	5–10	Goe.
YTG a	Grass lawn	90	-	-	<5	<3	10	Gyp.
YTG b	Grass lawn	85–90	<0.5	-	<5	<3	5–10	-
Nir Etsion								
Sample	**Type**	**Quartz**	**Calcite**	**Dolom.**	**K-Felds.**	**Plagioc.**	**Phyllos.**	**Others**
0–20 cm								
NE a	Banana 1	40	10	<0.5	<3	<3	40	Goe.
NE b	Banana 2	45	20	<1	5	<5	30	-
NE c	Banana 3	40	5–10	<1	5	5	45	Goe.
NE d	Olive 1	45	15	-	<3	<5	30–35	Goe. Am.
NE e	Olive 2	40–45	15	<0.5	<5	<5	35–40	-
NE f	Field 1	40	15	<0.5	<5	5	35–40	Goe.
NE g	Field 2	40	15	<0.5	<5	<5	35–40	-
NE h	Field 3	45	15	-	<3	<5	35	-
20–40 cm								
NE i	Banana 1	35–40	10	-	5	5	40–45	Am.
NE j	Banana 2	45	20	-	<5	<3	30	-
NE k	Banana 3	40–45	5–10	<3	<5	5	45	Am.
NE l	Olive 1	40–45	15	-	<5	5	40–45	-
NE m	Olive 2	40	15	<1	5	<3	35–40	-
NE n	Field 1	40	15	-	5	<5	35–40	Goe.
NE o	Field 2	35–40	15	-	5	5	40–45	Goe.
NE p	Field 3	40–45	25	?	<3	<3	30–35	Goe.
Sarid								
Sample	**Type**	**Quartz**	**Calcite**	**Dolom.**	**K-Felds.**	**Plagioc.**	**Phyllos.**	**Others**
0–20 cm								
F1 0–20	Fallow	30	20	-	?	<5	45	-
F2 0–20	Fallow	25	20–25	<3	5	5	45	Am.
F3 0–20	Fallow	25	20–25	<1	<3	<3	50	-
A	ECK	25–30	20	-	<5	<3	45–50	-
B	ECK	25–30	20–25	<1	?	?	45–50	-
C	ECK	25–30	20	<1	<3	<3	45–50	-
20–40 cm								
F1 20–40	Fallow	25–30	20	-	-	<5	50	-
F2 20–40	Fallow	25–30	20–25	-	<5	5	50	-
F3 20–40	Fallow	25–30	20–25	-	-	<3	50	-
D	ECK	25	20	-	5	<5	50–55	-
E	ECK	25–30	20–25	-	<3	<3	50	-
G	ECK	25–30	20	-	<3	-	50	-

ECK = Effluent + Compost + KCl; Abbreviations: dolom. = dolomite, K-felds. = K-feldspar; Plagioc. = plagiocalase; Phyllos. = phyllosilicates; Cli. = clinoptilolite; Am. = amphibole; Gyp. = gypsum; Goe. = goethite; ? = suspected.

3.2. Chemical Composition

The bulk chemical composition (Table 4) essentially reflects the mineralogical composition: the higher the quartz, the higher the SiO_2, and the higher the phyllosilicates, the higher the Al_2O_3. Thus, the sandy Mishmeret soil has the highest average SiO_2 concentration of 90% and the lowest Al_2O_3 concentration of 4.0%. The clayey Sarid soil has the lowest average SiO_2 concentration of 43% and the highest Al_2O_3 concentration of 11%. This relationship is not straightforward, as phyllosilicates also comprise SiO_2, which is higher in smectitic IS than in illitic IS or kaolinite. Thus, Gilat and Bet Dagan soils have the same average SiO_2 concentration of 63% but different quartz amounts due to the higher phyllosilicate amount and the smectitic nature of the IS in Bet Dagan. CaO directly reflects the amount of calcite, as its concentration in phyllosilicates and plagioclase is rather marginal, and the amount of dolomite is negligible. Fe_2O_3 is strongly associated with phyllosilicates, as indicated by its correlation with Al_2O_3 (Figure 4). The K_2O average concentration K_2O is 1.1%–1.2% in four sites, indicating K is rather stable in the clayey soils studied, whereas in the Mishmeret sandy soil, it is 0.6%. The K_2O correlation with Al_2O_3 (Figure 5) exhibits a complex behavior that is discussed below.

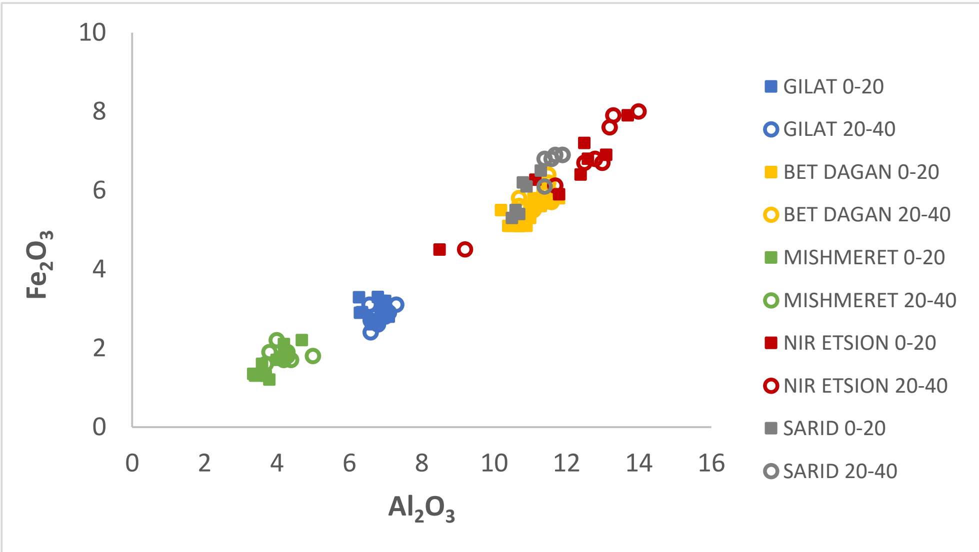

Figure 4. A plot of F_2O_3 versus Al_2O_3 in all bulk samples with a positive correlation trendline of y = 0.5993x − 0.867, and R^2 = 0.965.

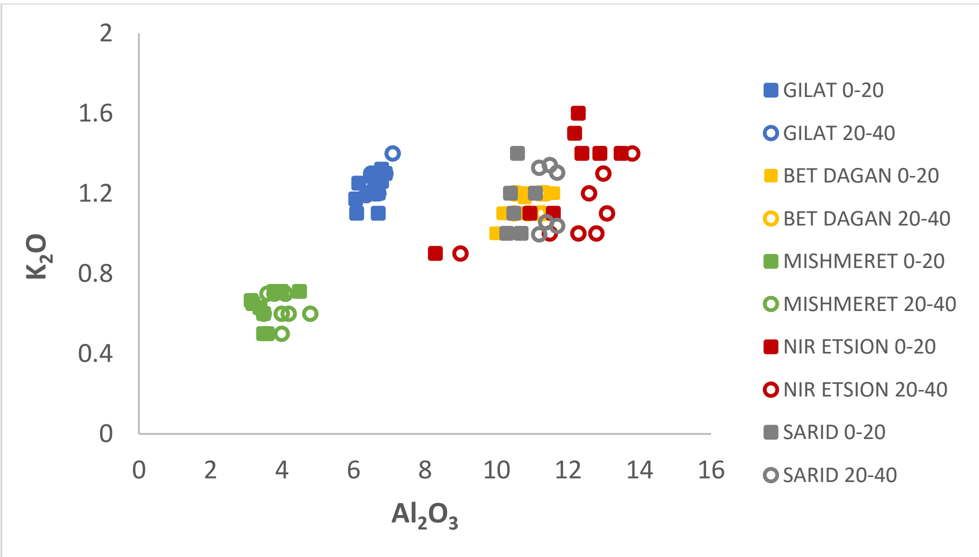

Figure 5. A plot of K_2O versus Al_2O_3 in all bulk samples. The Gilat site is out of the trend line as it is associated with both the 2:1 phyllosilicates and K-feldspars of a higher K_2O/Al_2O_3 ratio.

Table 4. Chemical composition (w/w %).

(4a) Gilat								
0–20								
	F 0-20	**F1 0-20**	**F2 0-20**	**D**	**G**	**J**	**A**	**C**
SiO_2	59.4	60.7	61.9	65.2	64.6	64.6	62.5	65.0
Al_2O_3	6.9	6.4	6.3	6.7	6.9	7.0	6.9	6.3
Fe_2O_3	3.3	3.0	3.4	2.8	3.2	2.9	3.1	3.0
TiO_2	0.8	0.8	0.7	0.8	0.8	0.8	0.8	0.8
CaO	13.2	12.0	11.9	10.1	10.1	10.2	11.3	10.0
MgO	2.0	1.9	1.8	1.7	1.7	1.8	1.8	1.6
MnO	0.05	0.1	0.1	0.05	0.06	0.06	0.05	0.05
Na_2O	0.7	0.8	0.8	0.7	0.9	0.9	0.8	0.7
K_2O	1.2	1.3	1.2	1.2	1.2	1.3	1.1	1.1
P_2O_5	0.1	0.1	<0.1	0.1	0.1	0.2	0.1	0.2
SO_3	<0.1	<0.1	<0.1	<0.1	<0.1	<0.1	<0.1	<0.1
LOI	12.8	12.7	12.5	10.6	10.1	10.3	11.9	10.9
Total	100.5	99.7	100.5	100.0	99.7	100.0	100.4	99.7
	H	**L**	**N**	**B**	**I**	**K**	**M**	
SiO_2	64.5	63.5	62.2	63.8	63.8	65.0	64.1	
Al_2O_3	6.9	6.9	7.1	6.6	6.8	6.9	7.0	
Fe_2O_3	2.9	2.9	2.9	2.7	3.4	3.3	3.3	
TiO_2	0.8	0.8	0.8	0.8	0.8	0.8	0.8	
CaO	10.3	10.4	11.5	10.5	10.2	9.9	9.7	
MgO	1.7	1.8	1.9	1.7	1.7	1.7	1.7	
MnO	0.06	0.06	0.06	0.05	0.06	0.06	0.06	
Na_2O	0.9	0.9	0.8	0.8	0.9	0.9	0.9	
K_2O	1.3	1.3	1.3	1.2	1.2	1.2	1.3	
P_2O_5	0.2	0.2	0.2	0.2	0.2	0.2	0.2	
SO_3	<0.1	<0.1	<0.1	<0.1	<0.1	<0.1	<0.1	
LOI	10.5	10.6	11.5	11.1	10.8	10.0	10.3	
Total	100.0	99.3	100.3	99.5	99.9	100.0	99.4	
20–40								
	F 20-40	**F1 20-40**	**F2 20-40**	**Q**	**R**	**U**	**P**	
SiO_2	59.2	62.0	60.8	59.2	63.9	64.0	61.4	
Al_2O_3	6.8	6.6	6.6	6.9	6.7	7.0	6.6	
Fe_2O_3	2.8	2.8	3.2	2.9	2.9	3.1	2.5	
TiO_2	0.8	0.8	0.8	0.8	0.8	0.9	0.8	
CaO	13.4	11.5	12.2	13.3	11.1	10.2	12.4	
MgO	1.8	1.7	1.9	1.8	1.7	1.7	1.7	
MnO	0.06	0.1	0.1	0.06	0.05	0.06	0.05	
Na_2O	0.8	0.8	0.8	0.6	0.6	0.6	0.6	
K_2O	1.2	1.2	1.2	1.2	1.3	1.3	1.2	
P_2O_5	0.1	0.1	0.1	0.1	0.1	0.2	0.1	
SO_3	<0.1	<0.1	<0.1	<0.1	<0.1	<0.1	<0.1	
LOI	13.3	11.9	12.5	12.9	11.0	10.8	12.1	
Total	100.3	99.5	100.1	99.8	100.2	99.9	99.5	

Table 4. *Cont.*

	S	W	Y	O	T	V	X
SiO_2	63.0	63.5	61.0	63.3	63.0	64.0	64.0
Al_2O_3	7.0	7.0	7.1	6.9	6.8	7.0	7.3
Fe_2O_3	3.0	3.1	3.0	3.1	2.7	2.9	3.2
TiO_2	0.9	0.9	0.8	0.8	0.8	0.9	0.9
CaO	10.6	10.5	11.9	10.7	10.8	10.4	10.0
MgO	1.8	1.7	1.8	1.7	1.7	1.7	1.7
MnO	0.06	0.06	0.06	0.06	0.06	0.06	0.06
Na_2O	0.6	0.7	0.6	0.7	0.6	0.6	0.6
K_2O	1.3	1.3	1.3	1.3	1.3	1.3	1.4
P_2O_5	0.2	0.2	0.2	0.2	0.2	0.2	0.2
SO_3	<0.1	<0.1	<0.1	<0.1	<0.1	<0.1	<0.1
LOI	11.7	10.5	12.0	10.9	11.5	10.7	10.4
Total	100.2	99.5	99.8	99.7	99.5	99.8	99.8

(4b) Bet Dagan

0–20

	F1	F2	F3	A	B	G	J	K	C	D
SiO_2	62.6	62.0	61.9	63.1	62.6	62.9	63.4	63.6	61.6	64.3
Al_2O_3	11.1	11.0	11.0	10.5	10.4	11.0	10.9	10.8	10.2	10.5
Fe_2O_3	5.6	5.5	5.4	5.4	5.2	5.7	5.4	5.5	5.6	5.2
TiO_2	1.3	1.2	1.3	1.2	1.2	1.3	1.3	1.4	1.2	1.3
CaO	5.8	6.5	6.1	5.8	5.8	5.9	6.0	5.8	5.8	5.2
MgO	1.6	1.7	1.7	1.5	1.5	1.7	1.7	1.7	1.5	1.4
MnO	0.12	0.10	0.12	0.11	0.10	0.12	0.12	0.12	0.10	0.11
Na_2O	0.5	0.4	0.5	0.5	0.4	0.5	0.5	0.5	0.4	0.4
K_2O	1.2	1.1	1.2	1.1	1.1	1.1	1.1	1.2	1.0	1.1
P_2O_5	0.2	0.1	0.2	0.1	0.1	0.1	0.1	0.2	0.2	0.2
SO_3	<0.1	<0.1	<0.1	<0.1	<0.1	<0.1	<0.1	<0.1	<0.1	<0.1
LOI	9.8	10.2	10.0	10.8	11.2	9.4	8.9	9.1	11.8	9.7
Total	99.8	99.8	99.4	100.1	99.6	99.7	99.4	99.9	99.4	99.4
	H	**I**	**L**	**M**	**N**	**O**	**V**	**W**	**Y**	**Z**
SiO_2	62.1	62.0	63.4	64.2	63.7	64.9	63.6	61.5	64.4	64.4
Al_2O_3	11.8	11.3	10.8	10.9	10.7	10.8	10.7	11.1	10.7	10.7
Fe_2O_3	5.9	5.7	5.3	5.2	5.2	5.4	5.2	5.9	5.2	5.2
TiO_2	1.4	1.4	1.4	1.4	1.3	1.4	1.3	1.3	1.3	1.3
CaO	6.0	5.5	6.0	5.4	5.8	5.5	6.0	6.4	5.3	5.3
MgO	1.7	1.7	1.6	1.6	1.6	1.5	1.5	1.6	1.5	1.5
MnO	0.13	0.13	0.12	0.12	0.12	0.12	0.12	0.13	0.12	0.12
Na_2O	0.4	0.4	0.5	0.5	0.6	0.5	0.5	0.5	0.5	0.5
K_2O	1.2	1.2	1.2	1.2	1.1	1.2	1.1	1.2	1.2	1.2
P_2O_5	0.2	0.2	0.2	0.2	0.2	0.2	0.2	0.2	0.2	0.2
SO_3	<0.1	<0.1	<0.1	<0.1	<0.1	<0.1	<0.1	<0.1	<0.1	<0.1
LOI	9.4	9.9	9.0	8.8	9.1	8.7	9.9	10.0	9.3	9.3
Total	100.2	99.4	99.5	99.5	99.4	100.2	100.1	99.8	99.7	99.7

Table 4. *Cont.*

	20–40										
	F1 20-40	**F2 20-40**	**F3 20-40**	**P**	**Q**	**R**	**S**	**T**	**AB**	**AC**	**AD**
SiO_2	60.7	60.4	60.5	62.5	64.0	64.6	64.3	62.0	61.5	64.1	60.6
Al_2O_3	11.5	11.6	11.6	11.4	10.8	10.7	10.7	11.5	11.5	10.7	11.4
Fe_2O_3	6.5	5.9	5.8	5.8	5.4	5.7	5.3	6.3	6.0	5.9	6.1
TiO_2	1.3	1.3	1.3	1.3	1.3	1.3	1.3	1.3	1.3	1.3	1.3
CaO	6.3	6.5	6.5	6.1	5.9	5.4	5.4	5.6	6.5	5.7	6.2
MgO	1.7	1.7	1.7	1.7	1.6	1.5	1.5	1.6	1.7	1.5	1.7
MnO	0.13	0.12	0.13	0.12	0.12	0.12	0.12	0.12	0.13	0.12	0.13
Na_2O	0.3	0.3	0.4	0.3	0.3	0.3	0.3	0.3	0.6	0.6	0.5
K_2O	1.2	1.2	1.2	1.1	1.2	1.2	1.2	1.2	1.1	1.1	1.2
P_2O_5	0.2	0.2	0.2	0.2	0.2	0.2	0.2	0.2	0.2	0.2	0.2
SO_3	<0.1	<0.1	<0.1	<0.1	<0.1	<0.1	<0.1	<0.1	<0.1	<0.1	<0.1
LOI	10.2	10.3	10.2	9.5	9.1	9.1	9.2	9.6	9.8	9.0	10.7
Total	100.0	99.5	99.5	100.0	99.9	100.1	99.5	99.7	100.3	100.2	100.0

(4c) Mishmeret.

		0–20						5–20	
	YTF	**YT a**	**YTFb**	**YT-1**	**YT-1a**	**YT-1b**	**YTG**	**YTGa**	**YTGb**
SiO_2	90.5	91.1	92.0	88.8	89.7	88.2	89.0	88.5	89.8
Al_2O_3	3.4	3.6	3.4	4.2	4.0	4.7	3.8	3.7	3.7
Fe_2O_3	1.5	1.7	1.4	2.2	1.8	2.3	1.3	1.4	1.4
TiO_2	0.3	0.3	0.2	0.5	0.5	0.5	0.3	0.5	0.3
CaO	0.7	0.7	0.5	0.7	0.6	0.6	0.7	0.6	0.8
MgO	0.3	0.3	0.2	0.3	0.3	0.3	0.2	0.2	0.2
MnO	0.0	0.0	0.0	0.0	0.0	0.0	0.0	0.0	0.0
Na_2O	0.3	0.2	0.3	0.3	0.2	0.2	0.2	0.2	0.2
K_2O	0.7	0.6	0.7	0.7	0.7	0.7	0.5	0.6	0.5
P_2O_5	0.1	< 0.1	$\leq$ 0.1	0.2	0.2	0.2	<0.1	<0.1	<0.1
L.O.I.	2.1	1.8	1.7	2.6	2.4	2.6	3.7	3.7	3.0
Total	99.8	100.4	100.4	100.4	100.4	100.3	99.7	99.4	99.9

					20–40				
	YTF 20-40	**YTFa 20-40**	**YTFb 20-40**	**YT-1**	**YT-1a**	**YT-1b**	**YTG**	**YTGa**	**YTGb**
SiO_2	89.2	89.7	90.8	89.0	90.0	88.7	89.4	88.3	90.5
Al2O_3	4.3	4.2	3.7	4.0	3.8	4.3	4.4	5.0	4.2
Fe_2O_3	1.9	1.9	1.7	2.3	2.0	2.0	1.8	1.9	1.8
TiO_2	0.4	0.4	0.3	0.4	0.5	0.5	0.4	0.5	0.3
CaO	0.6	0.5	0.5	0.6	0.5	0.7	0.5	0.5	0.4
MgO	0.3	0.3	0.2	0.3	0.2	0.3	0.2	0.2	0.2
MnO	0.0	0.0	0.0	0.0	0.0	0.0	0.0	0.0	0.0
Na_2O	0.4	0.3	0.3	0.3	0.3	0.3	0.2	0.2	0.1
K_2O	0.7	0.6	0.6	0.7	0.7	0.7	0.6	0.6	0.5
P_2O_5	0.2	0.2	0.2	0.2	0.2	0.2	<0.1	<0.1	<0.1
L.O.I.	2.3	1.9	1.7	2.6	2.3	2.6	2.3	2.4	2.1
Total	100.3	100.0	100.0	100.4	100.5	100.3	99.8	99.6	100.0

Table 4. *Cont.*

(4d) Nir Etsion.								
0–20								
	NEa	**NEb**	**NEc**	**NEd**	**NEe**	**NEf**	**NEg**	**NEh**
SiO_2	54.5	56.2	57.5	50.9	52.6	51.4	51.9	50.5
Al_2O_3	13.1	8.5	13.7	11.8	11.1	12.6	12.4	12.5
Fe_2O_3	7.0	4.6	8.0	6.0	6.4	6.9	6.5	7.3
TiO_2	1.4	0.8	1.4	1.2	1.2	1.3	1.2	1.3
CaO	6.4	12.6	4.6	10.5	9.3	8.6	9.0	9.6
MgO	1.8	1.3	1.8	1.4	1.4	1.8	1.8	1.8
MnO	0.2	0.1	0.2	0.1	0.1	0.1	0.1	0.1
Na_2O	0.4	0.4	0.4	0.3	0.3	0.3	0.3	0.3
K_2O	1.4	0.9	1.4	1.1	1.1	1.4	1.5	1.6
P_2O_5	0.3	0.1	0.2	0.1	0.1	0.3	0.3	0.3
LOI	13.7	14.8	11.1	16.7	16.8	15.0	15.3	15.0
Total	100.1	100.4	100.2	100.1	100.4	99.6	100.4	100.2
20–40								
	NEi	**NEj**	**NEk**	**NEl**	**NEm**	**NEn**	**NEo**	**NEp**
SiO_2	55.5	56.5	57.0	54.4	52.5	50.8	52.0	45.3
Al_2O_3	13.2	9.2	14.0	13.0	12.5	12.8	13.3	11.7
Fe_2O_3	7.7	4.6	8.1	6.8	6.8	6.9	8.0	6.2
TiO_2	1.4	0.9	1.4	1.3	1.3	1.3	1.3	1.1
CaO	6.0	12.2	5.4	8.9	10.1	10.3	8.3	15.2
MgO	1.7	1.2	1.7	1.5	1.4	1.7	1.8	1.6
MnO	0.2	0.1	0.2	0.1	0.1	0.1	0.1	0.1
Na_2O	0.3	0.4	0.4	0.3	0.3	0.3	0.3	0.3
K_2O	1.3	0.9	1.4	1.0	1.0	1.2	1.1	1.0
P_2O_5	0.2	0.1	0.2	0.1	0.1	0.3	0.2	0.2
LOI	13.0	14.5	10.7	13.1	14.4	14.8	14.0	17.8
Total	100.4	100.5	100.4	100.5	100.5	100.4	100.4	100.5

(4e) Sarid.						
0–20						
	F1 0–20	**F2 0–20**	**F3 0–20**	**A**	**B**	**C**
SiO_2	42.4	42.3	42.3	44.2	42.0	42.0
Al_2O_3	10.5	10.9	10.7	11.3	10.6	10.8
Fe_2O_3	5.4	6.2	5.5	6.6	5.6	6.3
TiO_2	1.0	1.1	1.1	1.1	1.0	1.0
CaO	16.2	15.2	16.1	13.9	14.9	15.0
MgO	1.9	2.2	2.0	2.2	2.1	2.3
MnO	0.11	0.11	0.11	0.12	0.13	0.12
Na_2O	0.3	0.3	0.3	0.3	0.3	0.4
K_2O	1.0	1.0	1.1	1.2	1.2	1.4
P_2O_5	0.2	0.3	0.2	0.6	1.1	0.7
SO_3	<0.1	<0.1	<0.1	<0.1	<0.1	0.1
L.O.I	20.7	20.2	20.0	18.5	20.7	20.2
Total	99.7	99.8	99.4	100.0	99.6	100.3

Table 4. *Cont.*

	20–40					
	F1 20-40	**F2 20-40**	**F3 20-40**	**D**	**E**	**G**
SiO_2	47.3	46.1	45.3	47.1	46.0	46.4
Al_2O_3	11.9	11.6	11.4	11.9	11.4	11.7
Fe_2O_3	7.0	6.9	6.9	7.0	6.2	7.0
TiO_2	1.1	1.1	1.1	1.1	1.1	1.1
CaO	11.8	12.0	13.5	11.6	12.8	11.4
MgO	2.2	2.2	2.1	2.3	2.3	2.3
MnO	0.1	0.1	0.1	0.1	0.1	0.1
Na_2O	0.3	0.3	0.3	0.3	0.3	0.3
K_2O	1.0	1.1	1.0	1.3	1.3	1.3
P_2O_5	<0.1	0.1	0.1	0.4	0.6	0.4
SO_3	<0.1	<0.1	<0.1	<0.1	<0.1	<0.1
L.O.I	17.3	18.5	18.7	17.3	18.1	18.2
Total	100.0	100.0	100.4	100.4	100.0	100.3

Differences in the bulk chemical composition between fallow and cultivated plots are quite few. CaO decreases in cultivated soils due to irrigation. It is lower by 13% in Gilat, 8% in Bet Dagan, Nir Etzion, and Sarid's topsoils. Sarid is the only site where a decrease in CaO is distinguished in the subsoil.

In general, average K_2O concentrations are comparable in all sites between topsoil and subsoil and between fallow and cultivated soils. In Gilat, there is a minor rise of 4% in average K_2O concentration and K_2O/Al_2O_3 ratio, from topsoil to subsoil, which may be related to some clay eluviation. In Gilat, Bet Dagan, and Mishmeret, average K_2O concentrations for fallow and cultivated soils are comparable, but the lawn samples in Mishmeret show a remarkable decline of 24%. The K_2O concentrations in the banana plots in Nir Etzion are variable but on average they are higher than those in the olive grove in both depths (but lower than those in the wheat field topsoil). Though fertilization data on the wheat field are missing, the highest K_2O and P_2O_5 concentrations in its topsoil and a 27% K_2O depletion in the subsoil are evidence for fertilization during the growing season. Sarid is the only site where the cultivated soil is enriched by K_2O, with an average concentration higher than fallow by 24%. This is accompanied by an average P_2O_5 concentration, which is four times greater than that in the fallow soil due to fertilization and irrigation by the wastewater. Another noteworthy change in chemical composition is observed in Mishmeret, where Al_2O_3 is 10% higher in fertilized plots compared to fallow and lawn soils, suggesting a rise in phyllosilicate amount in both depths.

3.3. Clay Fraction Mineralogical Composition

The dominant phyllosilicate mineral is IS, and kaolinite is the secondary one in the four fine-textured soils (Table 5), as in most soils in Israel (examples in [41], where it is termed montmorillonite; [26]). In many of the sandy Mishmeret soil samples, however, kaolinite is the major mineral, like in some red sandy soils along the coastal plain [42]. The saddle value, which estimates the illite-like layers in the IS phases, is rather variable (Figure 2). The highest value, >1, indicating the highest amount of illitic layers, is in Mishmeret. It is 0.82–1 in Gilat, 0.49–0.76 in Sarid, 0.56–0.72 in Nir Etzion, and 0.31–0.55 in Bet Dagan. The amount of illite decreases from south to north: 5%–15% in Gilat, ~5% in Nir Etzion, and <5% in Bet Dagan and Sarid, excluding Mishmeret, where it is 10%–20%. Palygorskite is present only in Gilat (Figure 2) in amounts of 5%–15%. Chlorite is present in trace amounts (<5%) in the fine-textured soils, whereas in the sandy soil (Mishmeret), it is undetectable. The latter site is distinguished also by the presence of the rare mixed-layered mineral kaolinite–smectite (KaS), which has already been formerly recorded in small amounts in some well-leached red soils in Israel [32,43].

Table 5. Mineralogical composition of the clay fraction (<1 µm); semi-quantitative (%).

Gilat							
Sample	**IS**	**Saddle**	**Kaolinite**	**Illite ***	**Chlorite**	**Palygorskite**	**Quartz**
0–20 cm							
F 0-20	50–55	0.83	15–20	10	<3	15	?
F1 0-20	60–65	1	15–20	5–10	<3	10	-
F2 0-20	60–65	0.86	15–20	5–10	<3	10	-
D	50–55	0.98	25	5–10	<3	10	?
E	50–55	0.98	25	10	<3	10	?
G	55	0.95	20–25	5–10	<3	5–10	<1
J	50–55	0.92	25	10	<3	5–10	<1
A	55	0.93	20	10	<3	10	?
B	50	0.97	20–25	10	<3	10	?
C	50–55	0.93	20–25	10	<3	10	?
H	55	0.97	20–25	10	<3	5–10	?
I	50–55	0.94	25	5–10	<3	10	<1
K	55	0.92	20	10	<3	10	<1
L	50	1	20–25	10–15	<3	10	?
M	55	0.94	25	10	<3	5–10	-
N	50–55	0.99	20	5–10	<3	10–15	?
20–40 cm							
F 20-40	55	0.86	20	5–10	<3	10	?
F1 20-40	60-65	0.95	15–20	5–10	<3	10	?
F2 20-40	55	0.75	20	5–10	<3	10	?
Q	50	0.83	20–25	10–15	<3	10–15	-
R	50	0.86	20	10–15	<3	10	-
U	60	0.92	20	5	<3	10	-
O	50–55	0.9	20–25	10	<3	10	-
P	50	0.82	20	10	<5	10	<2
S	55	0.92	20	5–10	<3	10–15	?
T	50–55	0.88	20	10	<3	15	?
V	55-60	0.91	20	5	<3	10	?
W	45–50	0.87	20–25	10–15	<3	10–15	<2
Y	50–55	0.91	20	10	<3	10–15	?
Bet Dagan							
Sample	**IS**	**Saddle**	**Kaolinite**	**Illite**	**Chlorite**	**Quartz**	**Goethite**
0–20 cm							
F1 0-20	80–85	0.39	15	<3	<3	?	-
F2 0–20	80–85	0.53	10–15	<5	<3	?	?
F3 0–20	80–85	0.46	10	<5	<3	?	?
A	80	0.51	10–15	<5	<3	?	?
B	80	0.56	10–15	<5	<3	?	?
G	80	0.41	15	<5	<3	-	?
J	85	0.37	10–15	?	<3	-	?
K	80–85	0.44	10–15	?	<3	?	?
C	80–85	0.50	10–15	<5	<3	?	?
D	80	0.55	10–15	<3	<3	?	?
E	80–85	0.54	10	<5	<3	?	?
H	80–85	0.35	10–15	?	<3	?	-
I	85	0.45	10	<3	<3	?	?
L	80	0.38	10–15	<3	<3	<1	<3
M	80–85	0.41	10–15	<3	<3	?	?
N	80–85	0.39	10–15	<3	<3	?	?
O	80	0.38	15	<5	<3	?	?
V	80–85	0.46	10–15	<3	<3	-	?
W	80	0.44	15	<3	<3	-	-
Y	80–85	0.49	10–15	?	<3	-	?
Z	80–85	0.50	10–15	<3	<3	-	-

Table 5. *Cont.*

			Bet Dagan				
Sample	**IS**	**Saddle**	**Kaolinite**	**Illite**	**Chlorite**	**Quartz**	**Goethite**
			20–40 cm				
F1 20-40	80–85	0.50	10–15	<3	<3	<1	<3
F2 20-40	80–86	0.48	15	?	<3	?	?
F3 20-40	80–86	0.41	10–15	<3	<3	?	-
P	85	0.42	15	?	<3	-	-
Q	80	0.31	15	<3	<3	?	-
R	80–85	0.45	10–15	<3	<3	<1	<3
S	80–85	0.39	10–15	<3	<3	-	?
T	85	0.42	10–15	<3	<3	?	?
AB	85	0.47	10	?	<3	?	?
AC	85	0.48	10	?	<3	-	-
AD	85	0.44	10	?	<3	?	-
AE	80–85	0.51	10	<3	<3	<1	<3
AF	80	0.50	10–15	<3	<3	<1	<3
AG	80	0.45	10–15	<3	<3	<1	<3
			Mishmeret				
Sample	**IS**	**Saddle**	**Kaolinite**	**Illite ***	**KaS**	**Quartz**	**Goethite**
			0–20 cm				
YTF1 0-20	40	>1	35	15	~5	<1	<5
YTF1a 0-20	40	>1	40	15	~5	<1	<5
YTF1b 0-20	40	>1	35	15	~5	<1	<3
YT1	25	>1	45	20	~5	<3	~5
YT1a	25	>1	45	20	~5	<3	~5
YT1b	30	>1	40	20	~5	<3	~5
			5–20 cm				
YTG 5-20	55	>1	35	5–10	<5	<1	<3
YTG a 5-20	55	>1	35	5–10	<5	?	<3
YTG b 5-20	55–60	0.98	30–35	5–10	<5	?	<3
			20–40 cm				
YTF1 20-40	45	>1	40	10	~5	<1	<3
YTF1a 20-40	50	>1	35	10	~5	<1	<3
YTF1b 20-40	40	>1	40	15	~5	<1	<3
YT1	30	>1	45	15	~5	<3	~5
YT1a	25	>1	50	15	~5	<3	<5
YT1b	35	>1	40	15	~5	<3	~5
YTG	60	0.95	30–35	5–10	<5	<1	<3
YTG a	60	>1	30	5	<5	<1	<5
YTG b	60–65	>1	30	<5	<5	?	<5
			Nir Etsion				
Sample	**IS**	**Saddle**	**Kaolinite**	**Illite**	**Chlorite**	**Quartz**	**Goethite**
NE a	75	0.72	15	5	<3	?	?
NE b	75–80	0.68	10–15	5	<3	-	?
NE c	80	0.67	10–15	<5	<3	<1	?
NE d	75–80	0.72	10–15	<5	<5	<1	-
NE e	80	0.72	10–15	<5	?	<1	-
NE f	75–80	0.62	10–15	<5	<5	?	?
NE g	75–80	0.72	10–15	<5	<3	-	-
NE h	75	0.61	15	<5	<5	<1	<3

Table 5. *Cont.*

Nir Etsion							
Sample	**IS**	**Saddle**	**Kaolinite**	**Illite**	**Chlorite**	**Quartz**	**Goethite**
20–40 cm							
NE i	75	0.68	15	5–10	<5	<1	?
NE j	75–80	0.65	15	5	<5	<1	?
NE k	75	0.70	15	5	<3	?	-
NE l	75–80	0.67	10–15	<3	5	<1	?
NE m	75	0.57	15	5	<3	<1	?
NE n	75	0.61	15	<5	<5	?	?
NE o	80	0.56	15	<5	?	-	-
NE p	75	0.63	10–15	5	<5	?	-
Sarid							
Sample	**IS**	**Saddle**	**Kaolinite**	**Illite**	**Chlorite**	**Quartz**	**Goethite**
0–20 cm							
F1 0-20	85	0.66	10	<3	<3	?	?
F2 0–20	85	0.57	10–15	<5	<3	?	?
F3 0–20	85	0.65	10–15	<3	<3	-	-
A	80–85	0.64	10–15	<3	<3	-	?
B	85	0.67	10–15	<3	<3	-	-
C	85–90	0.76	10–15	<3	<3	-	-
20–40 cm							
F1 20-40	80	0.55	15	<5	<3	-	-
F2 20-40	80–85	0.50	15	<3	<3	-	-
F3 20-40	80–85	0.49	10–15	<3	<3	-	-
D	80–85	0.51	15	5	<3	?	-
E	80–85	0.50	10	<5	<3	?	-
G	80–85	0.59	10–15	<3	<3	-	-

* Illite +Illitic IS; ? = suspected.

The semi-quantitative composition of the clay fraction does not allow for the detection of changes between fallow and cultivated soil or between topsoil and subsoil in the Gilat and Bet Dagan experimental permanent plots. A slightly higher average illite amount in the banana plots than that of the olive grove and the wheat field is observed in Nir Etzion. In contrast, prominent changes are observed in Mishmeret, where the fallow soil has higher illite and kaolinite amounts relative to the other sites studied. The highest illite and kaolinite amounts occur in the heavily fertilized tomato plots, indicating that cultivation enhances the natural pedogenic processes. The grass lawn, however, has similar kaolinite but lower illite amounts than the fallow soil. In the three fertilization levels, illite is higher in the topsoil than in the subsoil.

3.4. Relative Quantitative Analysis of the Clay Fraction

The values of the three indicators, **%IS**, **cg**, and **% Ka**, described above in Material and Methods, were calculated for all samples and are presented in Table 6. The values of the three indicators in Gilat topsoil, where the clay fraction is dominated by illitic IS, are rather scattered (Figure 6). It might be, in part, an analytical issue, a consequence of the overlap of the main reflection of palygorskite with that of PCI. However, in the subsoil, the three indicators display a similar trend as follows: an increase from fallow to control and medium-level fertilized plots, and then a decrease in the **cg** and **%IS** values in the highly fertilized plots, suggesting that where plant growth was maximal, the K balance was negative.

Table 6. Relative quantitative indicator of the clay fraction that were calculated after decomposition by the DecomXR program.

Sample	Type	%Ka	cg °2θ	%IS
Gilat				
Sample	**Type**	**%Ka**	**cg °2θ**	**%IS**
0–20 cm				
F 0-20	Fallow	26.5	6.65	63.0
F1 0-20	Fallow	15.5	6.76	43.4
F2 0-20	Fallow	12.4	6.63	42.9
D	Control	16.9	6.64	49.8
E	Control	14.4	6.83	60.9
G	Control	15.7	6.35	40.0
J	Control	16.8	6.49	46.6
A	M0, N3	14.5	6.85	58.2
C	M2, N0	15.0	6.85	62.3
H	M2, N0	14.4	6.40	45.5
L	M2, N0	15.4	6.44	43.6
N	M2, N0	14.6	6.68	51.7
B	M2, N3	17.0	6.83	66.3
I	M2, N3	14.9	6.43	46.3
K	M2, N3	14.3	6.57	53.1
M	M2, N3	15.5	6.50	43.6
20–40 cm				
F 20-40	Fallow	13.1	6.64	47.4
F1 20-40	Fallow	12.2	6.58	40.1
F2 20-40	Fallow	12.8	6.48	45.8
Q	Control	14.4	6.52	52.4
R	Control	13.1	6.67	66.0
U	Control	15.4	6.65	73.4
P	M2, N0	16.0	6.62	56.8
S	M2, N0	14.5	6.69	68.7
W	M2, N0	13.7	6.64	59.1
Y	M2, N0	14.3	6.78	72.6
O	M2, N3	15.2	6.47	51.2
T	M2, N3	13.8	6.56	62.3
V	M2, N3	14.9	6.69	63.1
X	M2, N3	14.8	6.75	58.1
Bet Dagan				
Sample	**Type**	**%Ka**	**cg °2θ**	**%IS**
0–20 cm				
F1 0–20	Fallow	6.7	6.04	22.1
F2 0–20	Fallow	6.5	6.10	22.0
F3 0–20	Fallow	6.1	6.18	28.3
A	Control	6.3	6.01	21.7
B	Control	5.6	5.93	28.8
G	Control	6.2	5.74	24.4
J	Control	6.2	5.90	17.6
K	Control	6.6	6.15	28.0
C	N4, P4, K2	6.5	6.02	20.3
D	N4, P4, K2	6.4	6.03	20.0
H	N4, P2, K2	6.0	5.69	23.4
I	N4, P2, K2	6.0	5.64	19.2
L	N4, P3, K2	5.6	5.99	23.9
M	N4, P3, K2	6.8	5.79	20.2
N	N4, P3, K2	6.6	5.80	27.8
O	N4, P3, K2	6.3	5.79	28.5
V	N4, P4, K2 + M	6.1	5.65	15.7
W	N4, P4, K2 + M	7.2	5.83	21.5
Y	N4, P4, K2 + M	6.8	5.77	18.4
Z	N4, P4, K2 + M	6.2	5.70	14.0

Table 6. *Cont.*

Bet Dagan				
Sample	**Type**	**%Ka**	**cg °2θ**	**%IS**
		20–40 cm		
F1 20-40	Fallow	6.4	6.22	29.0
F2 20-40	Fallow	7.2	6.24	37.8
F3 20-40	Fallow	7.6	6.25	39.7
P	Control	5.9	6.09	38.6
Q	Control	7.0	6.19	34.5
R	N4, P3, K2	6.8	6.22	39.6
S	N4, P3, K2	6.4	6.22	29.0
T	N4, P2, K2	8.1	6.15	28.0
AB	N4, P4, K2 + M	7.3	6.31	29.6
AC	N4, P4, K2 + M	6.5	6.27	33.6
AD	N4, P4, K2 + M	7.0	6.17	28.6
Mishmeret				
Sample	**Type**	**%Ka**	**cg °2θ**	**%IS**
		0–20 cm		
YTF1 0-20	Fallow	35.8	7.23	65.0
YTF1a 0-20	Fallow	28.2	7.19	68.1
YTF1b 0-20	Fallow	37.3	6.99	59.3
YT1	Tomatoes	43.1	7.91	87.9
YT1a	Tomatoes	51.1	7.88	80.6
YT1b	Tomatoes	36.9	7.68	89.2
		5–20 cm		
YTG 5-20	Grass lawn	24.1	6.27	57.8
YTG a 5-20	Grass lawn	25.6	6.03	55.7
YTG b 5-20	Grass lawn	26.9	5.99	52.7
		20–40 cm		
YTF1 20-40	Fallow	37.0	6.28	56.5
YTF1a 20-40	Fallow	34.3	6.35	57.0
YTF1b 20-40	Fallow	45.8	6.63	52.5
YT1	Tomatoes	44.4	6.56	57.0
YT1a	Tomatoes	52.9	6.64	62.2
YT1b	Tomatoes	50.3	6.49	51.7
YTG	Grass lawn	28.6	6.05	53.9
YTG a	Grass lawn	30.9	6.13	52.4
YTG b	Grass lawn	25.7	6.27	64.8
Nir Etsion				
Sample	**Type**	**%Ka**	**cg °2θ**	**%IS**
		0–20 cm		
NE a	Banana 1	7.7	5.75	15.0
NE b	Banana 2	6.3	5.81	12.4
NE c	Banana 3	6.8	5.91	13.6
NE d	Olive 1	6.1	5.86	17.0
NE e	Olive 2	5.8	5.86	19.7
NE f	Field 1	7.1	5.95	23.6
NE g	Field 2	7.1	5.95	23.6
NE h	Field 3	6.5	6.05	22.0

Table 6. *Cont.*

		Nir Etsion		
Sample	**Type**	**%Ka**	**cg** °2θ	**%IS**
		20–40 cm		
NE i	Banana 1	8.5	6.70	32.5
NE j	Banana 2	8.1	6.84	25.7
NE k	Banana 3	8.4	6.83	26.9
NE l	Olive 1	7.1	6.23	28.8
NE m	Olive 2	7.2	6.30	27.7
NE n	Field 1	7.1	6.24	28.8
NE o	Field 2	7.1	6.23	24.6
NE p	Field 3	7.3	6.51	42.3
		Sarid		
Sample	**Type**	**%Ka**	**cg** °2θ	**%IS**
		0–20 cm		
F1 0–20	Fallow	5.6	5.79	29.7
F2 0–20	Fallow	5.1	5.80	26.5
F3 0–20	Fallow	5.7	6.06	28.8
A	ECK.	5.6	5.65	21.9
B	ECK.	4.7	5.67	24.0
C	ECK.	5.6	5.76	22.6
		20–40 cm		
F1 20-40	Fallow	5.7	6.02	31.6
F2 20-40	Fallow	5.8	6.17	34.2
F3 20-40	Fallow	5.8	6.20	34.4
D	ECK.	5.4	5.98	31.9
E	ECK.	6.3	6.21	26.5
G	ECK.	6.1	6.20	32.6

In Bet Dagan, the clay fraction is dominated by smectitic IS, and neoformation of smectite is evidenced by the **cg** indicator, whose values gradually decrease along with the level of fertilization in the topsoil (Figure 6). However, in the subsoil, it decreases from fallow to control plots but gradually increases with the level of fertilization. This increase is probably due to higher clay amount and lower permeability, which promote K trapping and absorption by the smectitic IS. As most K activity here occurs in the smectitic realm, the **%IS** values are rather low and uniform. However, in the highly fertilized plots, a decrease in the **%IS** values occurs in both depths due to the disintegration of the illitic IS into both smectite and kaolinite. The **%Ka** values decrease from fallow to control plots in both depths and gradually increase with the level of fertilization, mainly in the topsoil. This decrease suggests that irrigation here enhances the natural neoformation of smectitic IS at the expense of kaolinite and other minerals, but that fertilization promotes kaolinite formation.

The three indicators in the one-growth plots are first examined in the clayey soils of Nir Etzion and Sarid, which share similar properties with Bet Dagan (e.g., the same range of the **cg** values). The **cg** and **%IS** values in the topsoil of the Nir Etzion banana plots are similar to or lower than those of the olive grove and the wheat field (Figure 6). Both indicators increase in the subsoil of the three soil types, especially the **cg** of the banana plot. It is worth noting that the **%IS** indicator is the highest in the wheat field topsoil, along with the highest K_2O/Al_2O_3 values in this site. Though the fertilization schedule of the wheat field is unknown, it turns out that the K application was surplus. The **%Ka** values of the banana plots in both depths are higher than those of the olive grove and the wheat field, reflecting kaolinite neoformation due to the intensive irrigation.

The **cg** values in Sarid are higher in the subsoil than in the topsoil, indicating natural illitization is taking place in depth, as in Nir Etzion. The **cg** and **%IS** values in the topsoil of the orchard are lower than those of the fallow, suggesting a negative K-balance, whereas in the subsoil the %IS in the orchard is slightly lower, but the **cg** values are equal to those of the fallow, maintaining an almost neutral K balance in depth. The **%Ka** values are the lowest among all sites studied so no difference between the fallow and the cultivated plots in both depths is detectable.

The sandy Mishmeret soil is unique also for its three clay indicators (Figure 6). The **%Ka** values are the highest among the five sites studied, and in the tomato plot, they are ~25% higher than in the fallow soil in both depths, indicating that cultivation enhances the natural kaolinite neoformation. Comparably, the **%IS** values are the highest and increase in topsoil, along with **cg** values, from fallow to the tomato plot, but decrease in the grass lawn, as no K is added to it. The fallow values show that much of the illitization processes take place mostly at the topsoil, so in the subsoil, the **cg** pattern returns but that of the **%IS** does not.

Gilat

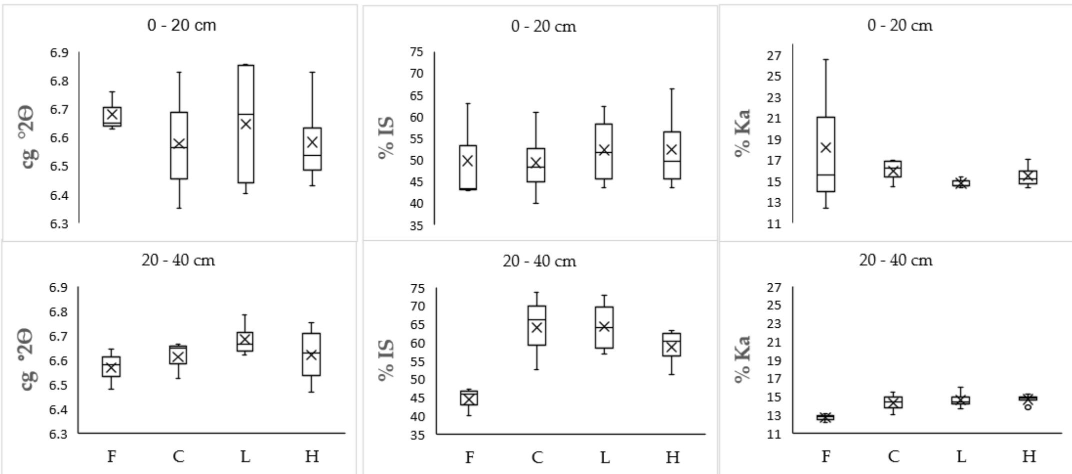

Bet Dagan

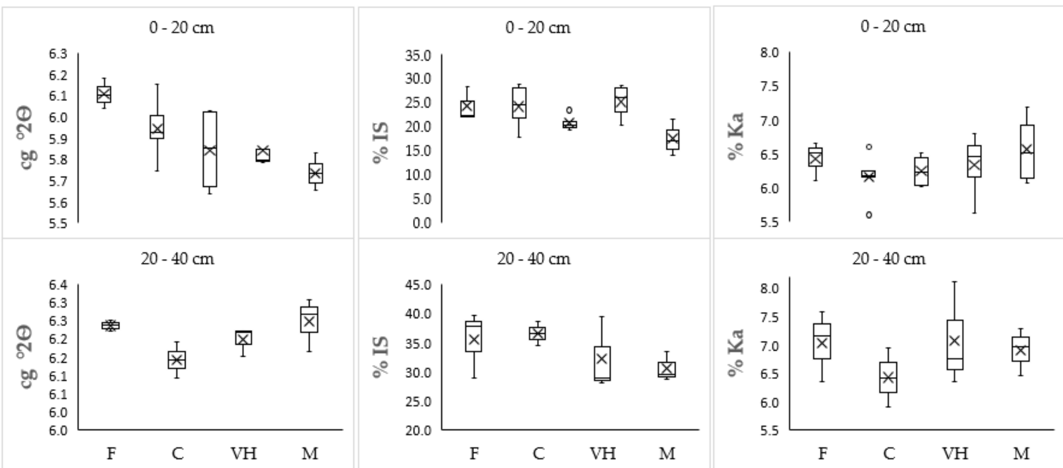

Figure 6. *Cont*.

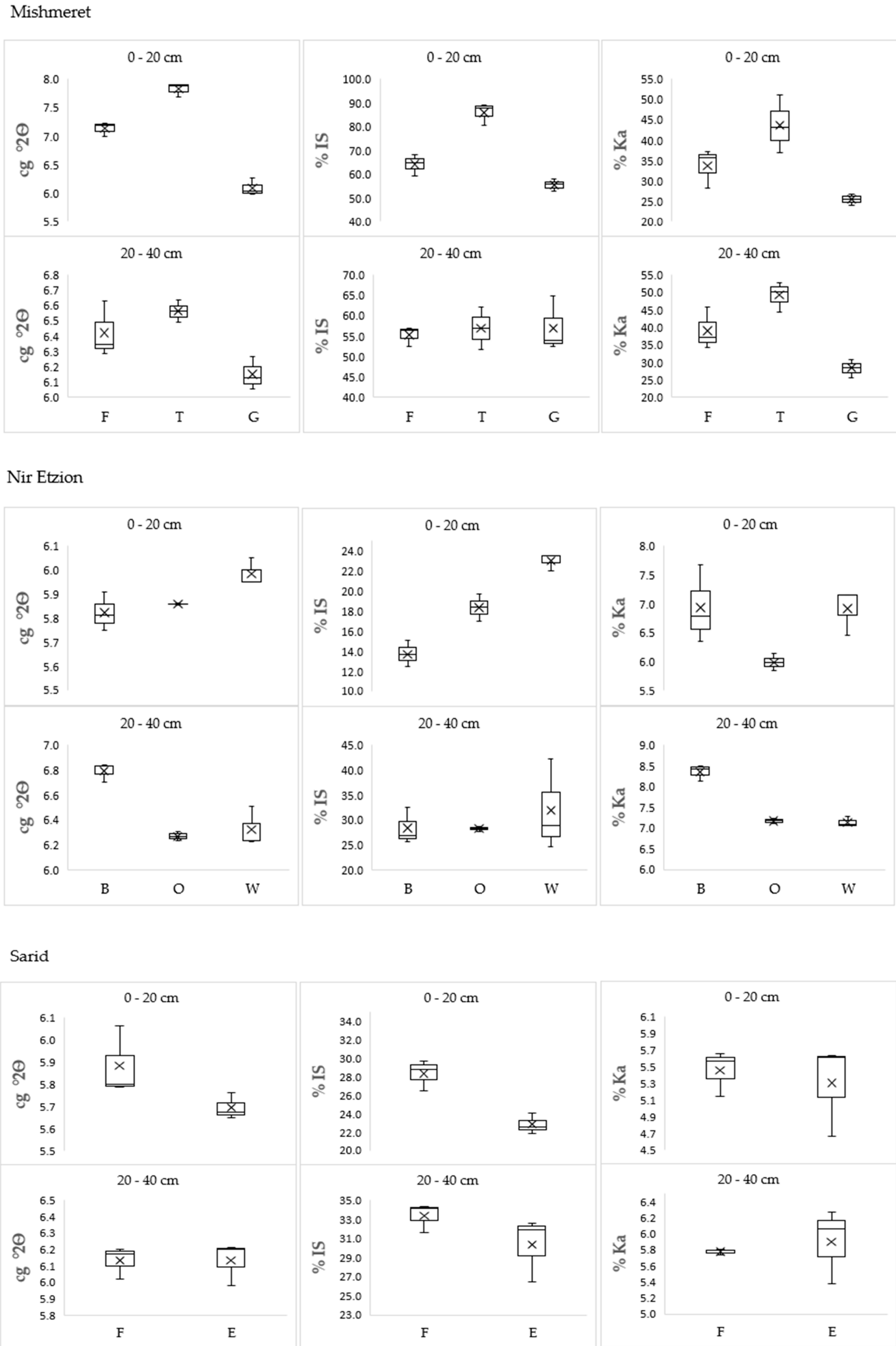

Figure 6. Diagrams of the three relative quantitative indicators, **cg**, **%IS**, and **%Ka**, used for evaluating the major potential changes in soil clay phyllosilicates due to cultivation. The x symbol is the average value. F = fallow; C = control; L = low fertilization level; H = high level; VH = very high level; M = manure; T = tomato; G = grass; B = banana; O = olive; W = wheat; E = effluents (wastewater).

In summary, the three indicators display a variety of responses to irrigation and fertilization. The effect of irrigation is evident in Gilat, Bet Dagan, and Mishmeret. A positive K balance due to K fertilization is evident by increased illitization in Bet Dagan, Mishmeret, and Nir Etzion's topsoils, whereas in Gilat and Sarid the K balance is negative. Enhancement of natural clay neoformation by cultivation is evident in Bet Dagan, Mishmeret, and Nir Etzion. A mutual increase in **%Ka** and **%IS** predominates in Mishmeret and occurs also in Gilat's subsoil.

4. Discussion

4.1. Composition of Lowland Soils—The Natural Processes

The natural processes that govern the original composition in each place are initially taken into consideration in order to study and comprehend potential changes in soil chemical and mineralogical composition produced by farming. The four fine-textured soils show a gradual compositional change from south to north that reflects both the increasing precipitation and the distance from nearby dust sources. Eventually, the regional geological and geomorphological conditions have an impact on each of them. Gilat's soil appears to be enriched by sand-sized quartz based on its texture and SiO_2 concentration, which are both roughly 20% higher than the typical concentration of northern Negev Holocene loess captured in archaeological sites [44]. This is caused by the addition of fine sand, winded from the neighboring sand dunes [45], which "dilutes" the loess. The amounts of calcite and feldspars (combined K-feldspar and plagioclase) in Gilat decrease from~20% for each mineral to ~10% in Bet Dagan. The feldspars' amount further decreases to $\leq$5% in Nir Etzion and almost vanishes in Sarid. Similarly, the quartz amount decreases from ~50% in Gilat to ~40% in Bet Dagan and Nir Etzion, and to ~30% in Sarid. The calcite amount, unpredictably, increases in the two latter sites. In Nir Etzion, it is probably due to a contribution of calcite from the limestone-built Mt. Carmel, where the colluvial soil is right at its foothill. It is questioned why the calcite at Sarid vertisol has increased further in comparison to nearby vertisols with 10% calcite [4,40]. The soft limestone outcrops above the orchard might be a local supply source.

In parallel to the general decrease in quartz, feldspars, and, in part, calcite, the amount of phyllosilicates increases from south to north. The amount of phyllosilicates increases from 15%–20% in Gilat to 40%–45% in Bet Dagan, 35%–45% in Nir Etzion, and reaches a maximum of ~50% in Sarid. This northward increase in the non-sandy soils is accompanied by changes in the clay fraction composition and, eventually, the phyllosilicates' assemblage.

The palygorskite in Gilat is mostly pedogenic, as its amount is higher than in dust [26]. Pedogenic palygorskite was documented earlier in similar Negev soils [46]. The most drastic changes occur between Gilat and Bet Dagan and include the disappearance of palygorskite, a drop in the amounts of illite and kaolinite, and the replacement of illitic IS by smectitic IS, as is evident by the saddle values. The amount of smectitic IS rises to >75% in Nir Etzion and Sarid, though the saddle values there are somewhat higher than those of Bet Dagan. Thus, the types and abundances of phyllosilicates also reflect long-term geologic factors, including the dissolution or alteration of primary feldspar and mica and the subsequent transformation and dissolution/precipitation reactions that operate within the soil horizons, as has been stated in another study in the USA [18].

The chemical composition reflects the reorganization of the bulk and clay fractions' mineralogical compositions. As has been noted earlier [32,47] the ratio of Fe_2O_3 to Al_2O_3 is mostly around 0.5–0.6 for the soil studied (Figure 4) and for all soils and surface sediments in Israel, indicating stability of both elements in the soil environment, which is also supported by trace concentrations in groundwater. The relations between K_2O and Al_2O_3 are complex (Figure 5) as neoformation of smectitic IS necessitates all Al_2O_3 and some K, whereas neoformation of kaolinite does not include K and the available K (as cation) may either adsorb to the 2:1 phyllosilicates or drain into groundwater. Thus, the range of K concentrations in Bet Dagan and Sarid is similar to that of Gilat, despite the significant increase in smectitic IS, reflecting the response of phyllosilicates to the local environmental condition. Potassium-rich minerals such as illite, illitic-IS, and K-feldspar dissolve and contribute a part of their K to the neoformed smectitic IS, confirming the importance of structural K release to pedogenic phyllosilicates [11–13].

Synthesizing all the trends of compositional changes described above suggests that the clayey nature of vertisols is not just a result of finning due to dust grain size decrease from south to north [48], or alluvial winnowing, but mainly due to the addition of neoformation phyllosilicates at the expense of quartz, feldspars, other primary minerals, and rain solutes. This process has been suggested for vertisols in Israel [29] and the USA [49].

Sandy soils like the Mishmeret soil react differently to the local environment due to their permeability. Soil K, derived from the decomposition of smectitic IS, supports the formation of pedogenic illite, as has been suggested for vegetation-rich soils [17,50]. This process has also been documented in several studies on well-leached red Mediterranean soils in Israel, e.g., [32,34]. The remaining SiO_2 and Al_2O_3 gradually form pedogenic kaolinite, which may turn into the main phyllosilicate. The occurrence of the minor but unique KaS mineral testifies to a transitional mineral through smectite-to-kaolinite weathering, as has been recorded in soils on limestone and other rocks under seasonal humid climates, e.g., [51,52]. Here, the high sand permeability compensates for the lower precipitation than in those humid occurrences and promotes KaS formation even under Mediterranean climate.

4.2. Effect of Irrigation

Irrigation can affect natural processes that are controlled by precipitation, such as the dissolution of relatively soluble minerals, or the transformation of phyllosilicates. The dissolution effect is evaluated here by comparing fallow and cultivated plots for calcite, as dolomite's amounts are too small. Dissolution of bedrock and dust calcite by rain in Mediterranean soils is a natural process [53–55] and is anticipated to be enhanced by adding irrigation waters. Fertilization and manure application can enhance this process owing to added acidity (e.g., ammonium sulfate), enhancing soil solution acidification (via nitrification) leading to calcite dissolution [56], and adding complexing ions (e.g., phosphate) [57]. This is best recorded by the mineralogical and chemical data (Tables 5 and 6) in the Gilat site where m.a.p. is about half of the other sites (Table 1). On the other end, the Mishmeret soil that developed under enhanced leaching conditions is completely calcite depleted, despite the fact that its parent material (dune sand and desert aeolian dust) contained substantial amounts of calcite [28,30]. The three vertisols are less well drained, especially the Sarid soil, and hence calcite dissolution is less pronounced.

Still, unpublished results of $CaCO_3$ measurements (estimated from the CO_2 volumes released using a calcimeter) from the Bet Dagan vertisol suggest that carbonates were lost from the topsoil during the about 30 years of experiments in five of the six experimental plots studied. The data from five fertilized soils for each sampling year were statistically weighed with respect to first measurement within each soil and subject to Anova analysis (Figure 7). This manipulation displays the decrease in calcite content in fertilized plots to be highly statistically significant ($p < 0.01$). The non-fertilized soil was excluded from this weighing manipulation because it showed almost no change in calcite content over the years.

Precipitation plays a major role in shaping the soil phyllosilicates' assemblages, as discussed in the previous section. It is therefore expected to enhance the transformation and neoformation of soil phyllosilicates, though the incorporation of fertilization may mask the net effect. The saddle values in Bet Dagan (Table 6) show enhanced smectitization of source phyllosilicates in the cultivated plots. In addition, the clear decline in the **cg** indicator between fallow and control plots in both depths suggests that smectitization is aided by the addition of irrigation water. The comparison between the rain-irrigated olive grove and the banana plot in Nir Etzion indicates that the kaolinite increase in the latter in both depths is a result of the heavy irrigation. In addition, the decrease in the **%IS** indicator in the topsoil, despite the heavy K fertilization has to be also attributed to irrigation. In contrast, the heavy irrigation of the grass loan in the sandy Mishmeret soil appears to be interfering with the natural production of kaolinite and illite IS. Instead, K concentration significantly decreases IS formation at the expense of illite and kaolinite.

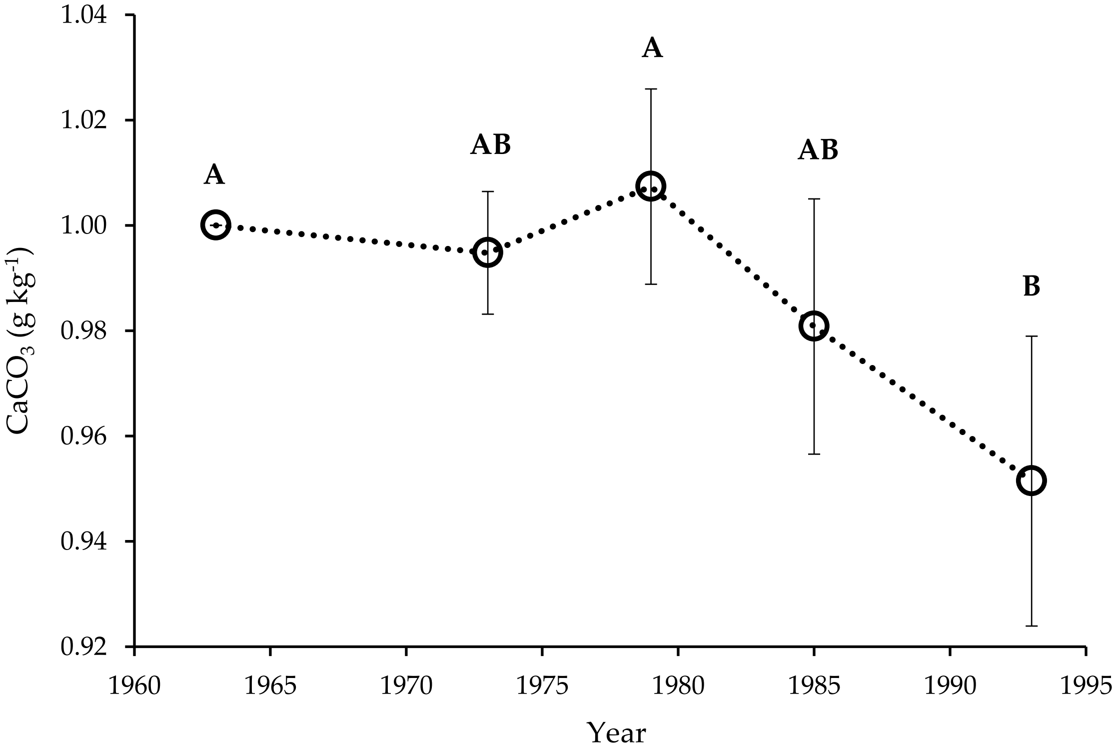

Figure 7. Anova analysis displays a gradual decrease in mean $CaCO_3$ concentrations in the topsoil of Bet Dagan permanent plots over the experiment years. Mean values denoted by same letters are not significantly different according to the Tukey–Kramer HSD multiple-range test.

To our knowledge, these aspects have not been reported earlier in studies that explored the effects of freshwater irrigation, as mostly they examined parameters such as soil fertility, structure, and organic matter concentration, e.g., [58,59].

4.3. Effect of Fertilization

The current study focuses on how K fertilizer affects soil K balance as indicated by the phyllosilicate indicators. An indirect impact on the phyllosilicates may also occur when fertilizers other than K cause high plant growth and, consequently, enhanced K uptake, as in the Gilat site. This site is dominated by illitic IS phases, as expressed by the highest saddle values, and the subsoil is the main arena for pedogenic processes, as stated above. Basic KCl was applied to all fertilization levels, namely, the control plots, as well as two levels of animal manure application, either alone or together with N (Table 2a). The substantial increase in the %IS indicator that occurred in the subsoil, from the fallow to the control plots (Figure 6) indicates that the K added was much more than needed by the plants, leading to its storage as illitic IS phases. No further change in that indicator occurred under the higher fertilization level, whereas under the highest level, it slightly decreased. The highest N levels caused the highest plant growth and enhanced K uptake beyond its application Table 75 in [36],) causing the transformation of the original illitic IS phases to less illitic ones. Overall, a neutral K balance, as compared to the fallow values, is recorded by the **%IS** indicator in the topsoil, whereas a slightly positive one is recorded in the subsoil.

Dissimilar K balances between topsoil and subsoil are also recorded in the Bet Dagan site, which is dominated by smectitic IS phases, as expressed by the lowest saddle values.

The major decline in the **cg** indicator from the fallow to the control plots in both depths is caused by soil K consumption, turning the smectitic IS into a more smectitic one (Figure 6). This is in accord with previous studies, which reported that cropping without K fertilization led to the formation of stable smectite in alluvium soil containing carbonates, e.g., [60]. Under a fertilization level of the same K but higher P levels, the slight gradual decline in the **cg** indicator also indicates higher plant growth, soil K-consumption, and a local negative K balance. However, it became, unexpectedly, even more negative in the topsoil under the addition of manure. This suggests enhanced downward migration of manure-K, as has been shown before, e.g., [61], and a build-up of a K reservoir in the subsoil. Overall, a negative K balance, as compared to the fallow values, is recorded in the topsoil and a neutral one is recorded in the subsoil. Dissimilarity between topsoil and subsoil may reflect, in addition to a reduction in permeability and downward migration, a difference in root activity with depth [62,63].

From the response of the Gilat and Bet Dagan experimental permanent plots to K fertilization over the course of more than thirty years, as expressed by the relative quantitative indicators, it can be deduced that the change in the soil K availability is rather minor. This is a consequence of two main factors: a. the high amount of K-bearing IS phases in the soils and b. the crop rotation system under the same fertilization regime that compensates between more and less K-consuming plants, and between plants of different root depths [36].

The three single-plant sites, which are heavily fertilized by K, display an intricate behavior with respect to K balance. K uptake and release in the Nir Etzion banana plantation are mainly reflected by the **cg** indicator (Figure 6); a neutral to negative K balance occurs in the topsoil, whereas the subsoil displays a neutral to positive K balance. Moreover, the higher average illite amount in both depths (Table 6) records pedogenic illite formation, apparently due to plant activity, as has been suggested before [50]. This dynamic K behavior in the banana plots, with the intensive application and consumption by the plants, is suggested to reflect seasonal changes along the growth cycle. Surplus K during K application time leads to illite formation, which seems to be rather stable [8]. Nevertheless, during maximum growth and fruit-bearing, the illitic IS is partially decomposed, resulting in an overall neutral to slightly negative K balance. Such seasonal variability in the composition of IS phases due to plant activities has been already recorded in previous studies [18,64,65]. Similarly, it is suggested that the highest **%IS** and K_2O/Al_2O_3 values in the wheat field topsoil, which clearly indicate K application in excess, is also a seasonal phenomenon, as it was sampled after the harvest and before the rainy season.

The Sarid grapefruit orchard is the only site with a distinctly higher K_2O concentration than the fallow soil, and with **cg** and **%IS** indicators (Figure 6) that apparently represent a negative to neutral K balance. This is suggested to reflect a seasonal imbalance due to a time gap between the K application when K temporarily occurs as a water-soluble and exchangeable ion and is later fixed by the IS phases. Despite the deep roots, the subsoil is more illitized than the topsoil, which is suggested to be associated with wastewater irrigation, which has been shown to enhance downward K migration [66,67]. It has also been shown in experiments with green-manure plants that even deep-rooting crops extract most of their K demand from the upper soil layers [60].

Though K leaching should be anticipated in permeable sandy soils, the heavy manure application in the Mishmeret site strengthens the natural process of pedogenic illitization of former IS phases. This is expressed mainly in the topsoil by significant illite formation, along with an increase in the **cg** and **%IS** values, much more than in the other sites. The small amount of the clay fraction enables an intense response to K addition and immediate new chemical equilibrium with respect to pedogenic illite, as has been modeled by [50]. K application to nearby sandy soil significantly increased corn yield even under high salinity levels, in contrast to fine-textured soils [68].

The mutual formation of pedogenic kaolinite and illite has not been modeled, or reported before, aside from in some cases in non-cultivated soils in Israel [32–34]. The unique positive correlation between the amounts of kaolinite and illite at Mishmeret (Figure 8), well demonstrates their mutual pedogenic formation.

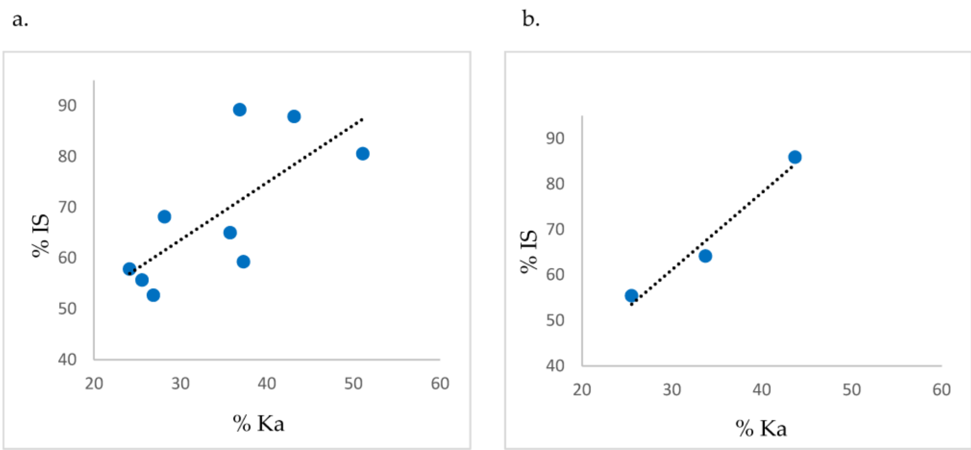

Figure 8. Plots of the **%Ka** indicator versus the **%IS** indicator in Mishmeret's topsoil: (**a**) all samples (R^2 = 0.526); (**b**) average values of the three levels of cultivation (R^2 = 0.966).

The main control on the small or undetectable modifications of phyllosilicates in the clayey soils after so many years of K application is the dominance of 2:1 phyllosilicates, which locally react to temporal changes in fertilization and plant growth. The dynamic K intake or uptake leads to a complex and heterogeneous clay assemblage at every depth within a profile [8,18]. Two additional controls are the crop rotation in the permanent plot experiments, as stated above, and proper fertilization scheme in the single-plant plots. These factors also probably hold for earlier studies that found that XRD patterns remained unaltered even after extensive cultivation [23,69,70].

5. Conclusions

Lowland long-term cultivated soils in Israel, four fine-textured and one sandy, were studied for the impact of K-fertilization and irrigation on their bulk mineralogical and chemical composition and the clay fraction mineralogical composition. The main conclusions are:

1. Natural changes in the composition of the clayey soils studied from the semi-arid to the Mediterranean climate regimes, from south to north, included reduced amounts of calcite, quartz, and feldspars and increased phyllosilicates. Mixed layer IS phases became more smectitic northward and palygorskite disappeared.
2. Application of K caused diverse behavior of the IS phases in the fine-textured soils. Quantitative XRD analysis estimated either a negative or a positive K balance in certain soil depths and fertilization levels at the same site. However, under high fertilization levels in the permanent plots, which led to high plant mass production and high K consumption, illitization declined.
3. Irrigation affected soils by dissolving calcite and transforming phyllosilicates, enhancing the smetitization of source IS phases at one site and kaolinite formation at another two sites.
4. The rather balanced K in the two permanent plot experiments after more than 30 years is due to the crop rotation applied and the dominance of IS phases in the clay fraction. The latter parameter is also the main reason for the small changes in K balance in the single-plant plots. This emphasizes the importance of IS minerals as a dynamic K pool that responds to plant needs.
5. An exceptional pedological system took place in the sandy soil with a small clay fraction, where kaolinite and illite amounts were higher than in the clayey soils.

Fertilization enhanced the natural process of contemporaneous transformation of source IS phases into both kaolinite and illite, resulting in a positive K balance.

Author Contributions: A.S.: Funding acquisition, Methodology, Formal analysis, Writing—original draft, and Visualization. P.F.: Funding acquisition, Resources, Visualization, and Writing—review and editing. A.B.-T.: Funding acquisition, Validation, and Writing—review and editing. All authors have read and agreed to the published version of the manuscript.

Funding: This study was funded by the Chief Scientist of the Ministry of Agriculture of Israel, grant No. 474-0002-07, and by the Geological Survey of Israel, to the three authors.

Data Availability Statement: No new data were created or analyzed in this study other than the presented results. Data sharing is not applicable to this article.

Acknowledgments: We acknowledge the funding support from the Chief Scientist of the Ministry of Agriculture of Israel, and acknowledge Geological Survey of Israel. D. Stiber, O. Yoffe, and S. Leizenbach (Geological Survey of Israel) for performing the chemical and mineralogical analyses. Four anonymous reviewers are thanked for their helpful comments and suggestions.

Conflicts of Interest: The authors declare no conflict of interest.

References

1. Huang, P. Chemistry of potassium in soils. In *Chemical Processes in Soils*; Tabatabai, M., Sparks, D., Eds.; Soil Science Society of America: Madison, WI, USA, 2005; pp. 227–292.
2. Simonsson, M.; Andersson, S.; Andrist-Rangel, Y.; Hillier, S.; Mattsson, L.; Öborn, I. Potassium release and fixation as a function of fertilizer application rate and soil parent material. *Geoderma* **2007**, *140*, 188–198. [CrossRef]
3. Zörb, C.; Senbayram, M.; Peiter, E. Potassium in agriculture–status and perspectives. *J. Plant Physiol.* **2014**, *171*, 656–669. [CrossRef] [PubMed]
4. Ravina, I.; Markus, Z. The effect of high exchangeable potassium percentage on soil properties and plant growth. *Plant Soil* **1975**, *42*, 661–672. [CrossRef]
5. Holthusen, D.; Peth, S.; Horn, R. Impact of potassium concentration and matric potential on soil stability derived from rheological indicators. *Soil Tillage Res.* **2010**, *111*, 75–85. [CrossRef]
6. Chen, Y.; Banin, A.; Borochovitch, A. Effect of potassium on soil structure in relation to hydraulic conductivity. *Dev. Soil Sci.* **1983**, *12*, 135–147.
7. Syers, J.K. Potassium in soils: Current concepts. In Proceedings of the IPI Golden Jubilee Congress, Feed the Soil to Feed the People: The Role of Potash in Sustainable Agriculture, Basel, Switzerland, 8–10 October 2002; pp. 301–310.
8. Bell, M.J.; Ransom, M.D.; Thompson, M.L.; Hinsinger, P.; Florence, A.M.; Moody, P.W.; Guppy, C.N. Considering Soil Potassium Pools with Dissimilar Plant Availability. In *Improving Potassium Recommendations for Agricultural Crops*; Murrell, T.S., Mikkelsen, R.L., Sulewski, G., Norton, R., Thompson, M.L., Eds.; Springer International Publishing: Cham, Switzerland, 2021; pp. 163–190.
9. Andrist-Rangel, Y.; Simonsson, M.; Andersson, S.; Öborn, I.; Hillier, S. Mineralogical budgeting of potassium in soil: A basis for understanding standard measures of reserve potassium. *J. Plant Nutr. Soil Sci.* **2006**, *169*, 605–615. [CrossRef]
10. Naumann, T.E.; Elliott, W.C.; Wample, J.M. K-Ar age constraints on the origin of micaceous minerals in Savannah River Site soils, South Carolina, USA. *Clays Clay Miner.* **2012**, *60*, 496–506. [CrossRef]
11. Bourbia, S.M.; Barré, P.; Kaci, M.B.N.; Derridj, A.; Velde, B. Potassium status in bulk and rhizospheric soils of olive groves in North Algeria. *Geoderma* **2013**, *197*, 161–168. [CrossRef]
12. Yuan, T.L.; Zelazny, L.W.; Ratanaprasatporn, A. Potassium status of selected Paleudults in the lower Coastal Plain. *Soil Sci. Soc. Am. J.* **1976**, *40*, 229–233. [CrossRef]
13. Pal, D.K.; Srivastava, P.; Durge, S.L.; Bhattacharyya, T. Role of weathering of fine-grained micas in potassium management of Indian soils. *Appl. Clay Sci.* **2001**, *20*, 39–52. [CrossRef]
14. Yanai, J.; Inoue, N.; Nakao, A.; Kasuya, M.; Ando, K.; Oga, T.; Takayama, T.; Hasukawa, H.; Takehisa, K.; Takamoto, A.; et al. Use of soil nonexchangeable potassium by paddy rice with clay structural changes under long-term fertilizer management. *Soil Use Manag.* **2023**, *39*, 785–793. [CrossRef]
15. Levy, G.J.; Bar-Tal, A. Alkali metals in soils. In *Encyclopedia of Soils in the Environment*, 2nd ed.; Goss, M., Oliver, M., Eds.; Elsevier: London, UK, 2023; Volume 2, pp. 116–125.
16. Barré, P.; Velde, B.; Catel, N.; Abbadie, L. Soil–plant potassium transfer: Impact of plant activity on clay minerals as seen from X-ray diffraction. *Plant Soil* **2007**, *292*, 137–146. [CrossRef]
17. Barré, P.; Velde, B.; Abbadie, L. Dynamic role of "illite-like" clay minerals: In temperate soils: Facts and hypotheses. *Biogeochemistry* **2007**, *82*, 77–88. [CrossRef]
18. Austin, J.C.; Richter, D.D.; Schroeder, P.A. Quantification of mixed-layer clays in multiple saturation states using NEWMOD2: Implications for the potassium uplift hypothesis in the SE United States. *Clays Clay Miner.* **2020**, *68*, 67–80. [CrossRef]

19. Ross, G.J.; Phillips, P.A.; Culley, J.L.R. Transformation of vermiculite to pedogenic mica by fixation of potassium and ammonium in a six-year field manure application experiment. *Can. J. Soil Sci.* **1985**, *65*, 599–603. [CrossRef]
20. Pernes-Debuyser, A.; Pernes, M.; Velde, B.; Tessier, D. Soil mineralogy evolution in the INRA 42 plots experiment (Versailles, France). *Clays Clay Miner.* **2003**, *51*, 577–584. [CrossRef]
21. Khormali, F.; Rezaei, F.; Rahimzadeh, N.; Hosseinifard, S.J.; Dordipour, E. Rhizosphere-induced weathering of minerals in loess-derived soils of Golestan Province, Iran. *Geoderma Reg.* **2015**, *5*, 34–43. [CrossRef]
22. Bain, D.C.; Griffen, D.T. Possible effects of land use on the clay mineralogy of a brown forest soil. *Clay Miner.* **2002**, *37*, 663–670. [CrossRef]
23. Tye, A.M.; Kemp, S.J.; Poulton, P.R. Responses of soil clay mineralogy in the Rothamsted Classical Experiments in relation to management practice and changing land use. *Geoderma* **2009**, *153*, 136–146. [CrossRef]
24. Barré, P.; Velde, B.; Fontaine, C.; Catel, N.; Abbadie, L. Which 2:1 clay minerals are involved in the soil potassium reservoir? Insights from potassium addition or removal experiments on three temperate grassland soil clay assemblages. *Geoderma* **2008**, *146*, 216–223. [CrossRef]
25. Paul, R.; Karthikeyan, K.; Vasu, D.; Sahoo, S.; Tiwary, P.; Gaikwad, S.S.; Chandran, P. Predicament in identifying clay palygorskite in Vertisols of Chhattisgarh basin, India. *Clay Res.* **2020**, *39*, 77–88. [CrossRef]
26. Sandler, A. Clay distribution over the landscape of Israel: From the hyper-arid to the Mediterranean climate regimes. *Catena* **2013**, *110*, 119–132. [CrossRef]
27. Yaalon, D.H.; Ganor, E. The influence of dust on soils during the Quaternary. *Soil Sci.* **1973**, *116*, 146–155. [CrossRef]
28. Dan, J. The effect of dust deposition on the soils of the land of Israel. *Quat. Int.* **1990**, *5*, 107–113. [CrossRef]
29. Yaalon, D.H.; Nathan, Y.; Koyumdjisky, H.; Dan, J. Weathering and catenary differentiation of clay minerals in soils on various parent materials in Israel. *Proc. Int. Clay Conf. Jerus.* **1966**, *1*, 187–198.
30. Dan, J. Soil chronosequences in Israel. *Catena* **1983**, *10*, 287–319. [CrossRef]
31. Verheye, W.H.; De La Rosa, D. Mediterranean soils. *Encycl. Land Use Land Cover Soil Sci.* **2009**, *7*, 96–120.
32. Sandler, A.; Meunier, A.; Velde, B. Mineralogical and chemical variability of mountain red/brown Mediterranean soils. *Geoderma* **2015**, *239–240*, 156–167. [CrossRef]
33. Tsatskin, A.; Sandler, A.; Porat, N. Toposequence of sandy soils in the northern coastal plain of Israel: Polygenesis and complexity of pedogeomorphic development. *Geoderma* **2013**, *197*, 87–97. [CrossRef]
34. Sandler, A.; Taitel-Goldman, N.; Ezersky, V. Sources and formation of iron minerals in eastern Mediterranean coastal sandy soils–A HRTEM and clay mineral study. *Catena* **2023**, *220*, 106644. [CrossRef]
35. Bergh, E.L.; Calderon, F.J.; Clemensen, A.K.; Durso, L.; Eberly, J.O.; Halvorson, J.J.; Jin, V.L.; Margenot, A.J.; Stewart, C.E.; Van Pelt, S.; et al. Time in a bottle: Use of soil archives for understanding long-term soil change. *Soil Sci. Soc. Am. J.* **2022**, *86*, 520–527. [CrossRef]
36. Bar-Yosef, B.; Kafkafi, U. *The Long-Term Permanent Plot Experiments in Israel*; The International Potash Institute: Zug, Switzerland, 2016.
37. Bar-Yosef, B.; Akiri, B. Sodium bicarbonate extraction to estimate nitrogen, phosphorus, and potassium availability in soils. *Soil Sci. Soc. Am. J.* **1978**, *42*, 319–323. [CrossRef]
38. Inoue, A.; Bouchet, A.; Velde, B.; Meunier, A. Convenient technique for estimating smectite layer percentage in randomly interstratified illite/smectite minerals. *Clays Clay Miner.* **1989**, *37*, 227–234. [CrossRef]
39. Lanson, B. Decomposition of experimental X-ray diffraction patterns (profile fitting): A convenient way to study clay minerals. *Clays Clay Miner.* **1997**, *45*, 132–146. [CrossRef]
40. Nachum, S.; Talesnick, M.; Weisberg, E.; Zaidenberg, R. Development of swelling induced shear and slickensides in Vertisols. *Geoderma* **2002**, *409*, 115629. [CrossRef]
41. Koyumdjiski, H.; Dan, J.; Soriano, S.; Nissim, N. *Selected Soil Profiles From Israel*; Volcani Center: Bet Dagan, Israel, 1988; 244p. (In Hebrew)
42. Singer, A. *The Soils of Israel*; Springer: Berlin, Germany; New York, NY, USA, 2007; 306p.
43. Sandler, A.; Avnaim-Katav, S. Unique clay assemblages in the Levant basin (Haifa Bay) subsurface reflect a land–sea transition zone and restricted environments throughout the last ~1 m.y. *Mar. Geol.* **2015**, *370*, 113–124. [CrossRef]
44. Lucke, B.; Sandler, A.; Vanselow, K.A.; Bruins, H.J.; Abu-Jaber, N.; Bäumler, R.; Porat, N.; Kouki, P. Composition of Modern Dust and Holocene Aeolian Sediments in Archaeological Structures of the Southern Levant. *Atmosphere* **2019**, *10*, 762. [CrossRef]
45. Crouvi, O.; Amit, R.; Enzel, Y.; Porat, N.; Sandler, A. Sand dunes as a major proximal dust source for late Pleistocene loess in the Negev Desert, Israel. *Quat. Res.* **2008**, *70*, 275–282. [CrossRef]
46. Yaalon, D.H.; Wieder, M. Pedogenic palygorskite in some arid brown (calciorthid) soils of Israel. *Clay Miner.* **1976**, *11*, 73–80. [CrossRef]
47. Haliva-Cohen, A.; Stein, M.; Goldstein, S.L.; Sandler, A.; Starinsky, A. Sources and transport routes of fine detritus material to the Late Quaternary Dead Sea basin. *Quat. Sci. Rev.* **2012**, *50*, 55–70. [CrossRef]
48. Dan, J.; Fine, P.; Lavee, H. *Soils of the Land of Israel*; The "ERETZ" Series Geographic Research & Publication; Tel Aviv University: Tel Aviv, Israel, 2007; 309p. (In Hebrew, with English summary)
49. Nordt, L.; Wilding, L.; Lynn, W.L.; Crawford, C. Vertisol genesis in a humid climate in the coastal plain of Texas, U.S.A. *Geoderma* **2004**, *122*, 83–102. [CrossRef]

50. Barré, P.; Berger, G.; Velde, B. How element translocation by plants may stabilize illitic clays in the surface of temperate soils. *Geoderma* **2009**, *151*, 22–30. [CrossRef]
51. Hong, H.; Churchman, G.J.; Gu, Y.; Yin, K.; Wang, C. Kaolinite–smectite mixed-layer clays in the Jiujiang red soils and their climate significance. *Geoderma* **2012**, *173*, 75–83. [CrossRef]
52. Oliveira, D.P.; Sartor, L.R.; Júnior, V.S.; Corrêa, M.M.; Romero, R.E.; Andrade, G.R.P.; Ferreira, T.O. Weathering and clay formation in semi-arid calcareous soils from Northeastern Brazil. *Catena* **2018**, *162*, 325–332. [CrossRef]
53. Stein, M.; Starinsky, A.; Katz, A.; Goldstein, S.L.; Machlus, M.; Schramm, A. Strontium isotopic, chemical, and sedimentological evidence for the evolution of Lake Lisan and the Dead Sea. *Geochim. Cosmochim. Acta* **1997**, *61*, 3975–3992. [CrossRef]
54. Fedoroff, N.; Courty, M.A. Revisiting the genesis of red Mediterranean soils. *Turk. J. Earth Sci.* **2013**, *22*, 359–375. [CrossRef]
55. Belmaker, R.; Lazar, B.; Stein, M.; Taha, N.; Bookman, R. Constraints on aragonite precipitation in the Dead Sea from geochemical measurements of flood plumes. *Quat. Sci. Rev.* **2019**, *221*, 105876. [CrossRef]
56. Tamir, G.; Shenker, M.; Heller, H.; Bloom, P.R.; Fine, P.; Bar-Tal, A. Dissolution and re-crystallization processes of active calcium carbonate in soil developed on tufa. *Soil Sci. Soc. Am. J.* **2012**, *76*, 1606–1613. [CrossRef]
57. Fine, P.; Mingelgrin, U. Release of phosphorus from waste-activated sludge. *Soil Sci. Soc. Am. J.* **1996**, *60*, 505–511. [CrossRef]
58. Nikolskii, Y.N.; Aidarov, I.P.; Landeros-Sanchez, C.; Pchyolkin, V.V. Impact of long-term freshwater irrigation on soil fertility. *Irrig. Drain.* **2019**, *68*, 993–1001. [CrossRef]
59. Rengasamy, P. Irrigation water quality and soil structural stability: A perspective with some new insights. *Agronomy* **2018**, *8*, 72. [CrossRef]
60. Tributh, H.V.; Boguslawski, E.V.; Lieres, A.V.; Steffens, D.; Mengel, K. Effect of potassium removal by crops on transformation of illitic clay minerals. *Soil Sci.* **1987**, *143*, 404–409. [CrossRef]
61. Hayashi, S.; Hara, M.; Katoh, M. Improvement on plant uptake of inorganic nutrients fertilized by migration of water-soluble organic matter from animal manure-based compost. *J. Soil Sci. Plant Nut.* **2022**, *22*, 3399–3413. [CrossRef]
62. Whitter, E.; Johansson, G. Potassium uptake from the subsoil by green manure crops. *Biol. Agric. Hortic.* **2001**, *19*, 127–141. [CrossRef]
63. Hinsinger, P.; Bell, M.J.; Kovar, J.L.; White, P.J. Rhizosphere processes and root traits determining the acquisition of soil potassium. In *Improving Potassium Recommendations for Agricultural Crops*; Murrell, T.S., Mikkelsen, R.L., Sulewski, G., Norton, R., Thompson, M.L., Eds.; Springer: Cham, Switzerland, 2021; pp. 99–117.
64. Turpault, M.P.; Righi, D.; Utérano, C. Clay minerals: Precise markers of the spatial and temporal variability of the biogeochemical soil environment. *Geoderma* **2008**, *147*, 108–115. [CrossRef]
65. Adamo, P.; Pierre, B.; Vincenza, C.; Bruce, V. Short term clay mineral release and re-capture of potassium in a Zea mays field experiment. *Geoderma* **2016**, *264*, 54–60.
66. Jalali, M.; Merikhpour, H.; Kaledhonkar, M.J.; Van Der Zee, S.E.A.T.M. Effects of wastewater irrigation on soil sodicity and nutrient leaching in calcareous soils. *Agric. Water Manag.* **2008**, *95*, 143–153. [CrossRef]
67. Arienzo, M.; Christen, E.W.; Quayle, W.; Kumar, A. A review of the fate of potassium in the soil–plant system after land application of wastewaters. *J. Hazard. Mater.* **2009**, *164*, 415–422. [CrossRef]
68. Bar-Tal, A.; Feigenbaum, S.; Sparks, D.L. Potassium-salinity interactions in irrigated corn. *Irrig. Sci.* **1991**, *12*, 27–35. [CrossRef]
69. Singh, B.; Goulding, K.W.T. Changes with time in the potassium content and phyllosilicates in the soil of the Broadbalk continuous wheat experiment at Rothamsted. *Eur. J. Soil Sci.* **1997**, *48*, 651–659. [CrossRef]
70. Velde, B.; Peck, T. Clay mineral changes in the Morrow Experimental Plots, University of Illinois. *Clays Clay Miner.* **2002**, *50*, 364–370. [CrossRef]